

ENCLAVES IN THE MT. PADBURY AND VACA
MUERTA MESOSIDERITES: MAGMATIC
AND RESIDUE (OR CUMULATE)
ROCK TYPES

Yukio IKEDA¹, Mitsuru EBIHARA² and Martin PRINZ³

¹*Department of Earth Sciences, Faculty of Science, Ibaraki University,
1-1, Bunkyo 2-chome, Mito 310*

²*Department of Chemistry, Faculty of Science, Tokyo Metropolitan University,
1-1, Fukazawa 2-chome, Setagaya-ku, Tokyo 158*

³*American Museum of Natural History, Central Park West at 79th Street,
New York, NY 10024, U. S. A.*

Abstract: Nine eucritic enclaves from mesosiderites and one possible enclave were petrologically and chemically studied. Three are from Mt. Padbury, six from Vaca Muerta, and one eucritic meteorite (AMNH 4627) was found in northern Chile and may be an enclave from Vaca Muerta. The enclaves studied were classified into two groups based on the presence or absence of primary ilmenite: (1) an Il-bearing group ranging in texture from medium-grained ophitic to coarse-grained gabbroic, and (2) an Il-free group from gabbroic to coarse-grained equigranular texture. Pigeonites of the Il-bearing group are more ferroan than those of the Il-free group. The peripheral portions of pigeonite in the Il-free group have remarkable textures not found in HED meteorites. They are replaced by more-magnesian hypersthene and troilite with a minor amount of silica-mineral, indicating that reduction of pigeonite took place by H₂S under subsolidus conditions prior to formation of the mesosiderite, metal-silicate mixing.

The major element compositions of the ten whole rock samples indicate that the Il-bearing group is similar to the non-cumulate eucrites, but the Il-free group differs from the cumulate eucrites. The Il-free group is significantly enriched in silica-mineral component in comparison with the cumulate eucrites. INAA and RNAA analyses for five whole rock samples were performed. Two Il-free enclaves have low REE contents with remarkable positive Eu-anomalies (chondrite-normalized Eu/Sm=13.6), and two Il-bearing enclaves have higher REE contents with slight positive Eu-anomalies (chondrite-normalized Eu/Sm=1.88–2.22). The high Eu/Sm ratios are partly due to terrestrial alteration of whitlockites, and the original Eu/Sm ratios of the Il-bearing and Il-free enclaves might be similar to those of non-cumulate eucrites and cumulate eucrites, respectively. These suggest that the Il-bearing enclaves were formed in the similar way to the non-cumulate eucrites, and the Il-free enclaves formed as cumulates from silica-rich magmas or as residues by partial melting of silica-bearing cumulate eucritic sources. A eucritic sample (AMNH 4627) has the highest REE content with no Eu-anomaly and is similar to the non-cumulate eucrites, and may be an independent eucrite.

1. Introduction

Silicate portions of the mesosiderites are very similar in bulk and mineral com-

positions to the howardites, except for the high silica and phosphorus contents in the former. This similarity suggests that mesosiderites may be a mixture of howardites and Fe-Ni metal and that the high silica contents of mesosiderite silicate portions could be explained by reduction of the ferromagnesian minerals by phosphorus which was originally included in Fe-Ni metal (DUKE and SILVER, 1967; FLORAN, 1978; SIMPSON and AHRENS, 1979; MITTFELDLT *et al.*, 1979; MITTFELDLT, 1979; DELANEY *et al.*, 1981; AGOSTO *et al.*, 1980; NEHRU *et al.*, 1980; HARLOW *et al.*, 1982).

The problem is that most mesosiderites have undergone thermal metamorphism which has made the original textures and mineral compositions of the silicate portions unclear. Fortunately, some mesosiderites include large eucritic enclaves which appear not to have suffered much recrystallization by the thermal metamorphism and reduction by the phosphorus in comparison with the matrix silicate portions of most mesosiderites. This is because of the large size (several cm in diameter) and the coarse-grained nature of these enclaves. The Mt. Padbury and Vaca Muerta mesosiderites are classified in the slightly-recrystallized subgroup of mesosiderites (POWELL, 1971; FLORAN, 1978), suggesting that the enclaves in these two mesosiderites may have escaped the metamorphic overprint. In order to clarify the differences in mineralogy and bulk chemistry between HED meteorites and eucritic enclaves in mesosiderites, we have studied nine eucritic enclaves from Mt. Padbury and Vaca Muerta and one possible enclave.

2. Samples and Analytical Procedures

2.1. Samples

The ten samples studied came from American Museum of Natural History, meteorite collection. Three are from Mt. Padbury, six from Vaca Muerta, and one eucritic sample (AMNH 4627) was found in northern Chile, where many specimens of the Vaca Muerta mesosiderite were recovered. It is surrounded completely by fusion crust and may have originally been an enclave in Vaca Muerta or an independent eucrite meteorite. This problem will also be discussed in this paper.

2.2. Electron-probe microanalyses

The chemical compositions of the constituent minerals were measured using an electron-probe microanalyser (EPMA). The accelerating voltage was 15 kV, the sample current from 3 to 10 nA, and the counting time was 10 s for the K-alpha line and background. The correction is by the Bence-Albee method for silicates, oxides, and phosphates and the standard ZAF method for sulfides and metals. The accuracy of minor elements such as MnO (less than 1 wt%) is about 0.1–0.2 wt%. Y_2O_3 and Ce_2O_3 contents of phosphates were measured with the sample current of 30 nA and counting time of 100 s for the peak and the background, and the detection limits (three sigma) of Y_2O_3 and Ce_2O_3 are 0.025 and 0.05 wt%, respectively.

2.3. Modal analyses and major element compositions

Modal analyses were performed, using an EPMA, by a step-scanning method which

measured the volume percents of plagioclase, high-Ca pyroxene, low-Ca pyroxene, silica-mineral, phosphate, and others (chromite, ilmenite, troilite, Fe-Ni metal, *etc.*). The high-Ca pyroxene includes exsolution lamellae in pigeonite as well as isolated augite grains. The point count number for each sample was about 2500, and the covered area about 0.5–1.0 cm².

Major element compositions of the silicate portions of each sample were calculated using the volume percent multiplied by the average composition of low-Ca pyroxene, high-Ca pyroxene, plagioclase, and silica-mineral (SiO₂=100 wt%) with presumed densities for each mineral. The results show that the total wt% of the silicate portions of the samples ranges from 93–98%. The “rests” are phosphates and non-silicate Fe phases such as chromite, ilmenite, troilite, and Fe-Ni metal.

2.4. Neutron activation analyses (NAA)

Samples were first nondestructively analyzed by instrumental NAA for Na, Sc, Cr, Fe, Co, Ni, and some rare earth elements (REEs). About 500 mg of grain samples were ground in a clean agate mortar to be made compositionally uniform. About 50 mg of each powdered sample was weighed and heat-sealed in a small plastic bag. JB-1, powdered standard rock sample supplied by the Geological Survey of Japan, and Allende powdered meteorite sample supplied by the Smithsonian Institution were used as standard references. Samples along with references were irradiated for 6 h in a neutron flux of 1.5×10^{12} n/cm² s at the Institute of Atomic Energy, Rikkyo University. After cooling for several days, gamma-ray intensities were measured with a pure Ge (coaxial-type) detector system in the inter-university laboratory at the Japan Atomic Energy Research Institute (JAERI) and at the Tokyo Metropolitan University. Measurements were repeated several times after appropriate cooling intervals. The data compiled by ANDO *et al.* (1987) for JB-1 and by JAROSEWICH *et al.* (1987) for Allende were used for final calculation.

To determine the precise abundances of REEs, radiochemical NAA (RNAA) was applied. About 50–70 mg of each powdered sample was sealed in clean, synthesized quartz tubing. Standard samples were prepared from pure chemical reagents. All the samples were irradiated at a neutron flux of 5×10^{13} n/cm² s for 6 h in the JRR-4 reactor of the JAERI. The analytical procedures applied were essentially the same as those described in EBHARA (1987).

3. Petrography

The ten samples studied show a wide variety of grain sizes, textures, and degrees of exsolution in pigeonites; these are summarized in Table 1. The modal compositions of the major silicate phases are tabulated in Table 2, and the mineral assemblages of each sample are shown in Table 3.

Primary ilmenite occurs in ferroan enclaves with *mg* values (MgO/(MgO+FeO) mole ratios) less than 0.46, and not in magnesian enclaves with *mg* values more than 0.47 (Tables 2 and 3). On the basis of the presence or absence of primary ilmenite, the samples studied are conveniently classified into two groups, the Il-bearing and Il-free groups. In Tables 1, 2, and 3, all samples are tabulated according to the classifi-

Table 1. Petrographic characteristics of the eucritic enclaves.

Enclave	Mesosiderite	Grain size	Texture	Exsolution	Replacement of Pig
Il-bearing enclaves					
Z	Mt. Padbury	medium	subophitic	weak	no
914	Vaca Muerta	coarse	gabbroic	moderate	no
4631	Vaca Muerta	medium	gabbroic-porphyritic	weak	no
4627	Vaca Muerta (?)	coarse	gabbroic	weak	no
U	Mt. Padbury	medium-coarse	subophitic-porphyritic	moderate	no
4632	Vaca Muerta	medium	subophitic-porphyritic	weak	no
Il-free enclaves					
4630	Vaca Muerta	coarse	gabbroic-granular	moderate	moderate
4633	Vaca Muerta	coarse	granular	moderate	weak
891	Vaca Muerta	coarse	gabbroic-granular	moderate	moderate-weak
H	Mt. Padbury	coarse	granular	moderate	remarkable

Degree of exsolution lamellae in pigeonite: weak—the width of lamellae is narrower than a few microns; moderate—the width is within the range from a few microns to 10 microns. Degree of replacement of pigeonite by hypersthene are shown: weak—a few % of pigeonites are replaced; remarkable—a few tens of % are replaced.

cation. In the following sections a brief petrography of each sample is given in the order of *mg* value (Table 2). Although three of the enclaves from Mt. Padbury were already studied mineralogically and petrologically by DELANEY *et al.* (1982) and MCCALL (1966), more-detailed petrography for each of them is given here.

3.1. Enclave Z from Mt. Padbury (*mg*=0.39, Il-bearing group)

Enclave Z has a medium-grained subophitic texture (Fig. 1), consisting mainly of plagioclase, pigeonite, and a silica-mineral (almost tridymite). Thin exsolution lamellae of augite are barely visible under the microscope. Ferroan olivine is rare and always occurs as small inclusions in pigeonite (Fig. 2). A zircon grain, about 10 microns across, was found as an irregularly-shaped grain associated with ilmenite (Fig. 3).

This enclave includes fine-grained aggregates, smaller than a few millimeters across (Fig. 4), where the main constituent minerals are troilite, augite, hypersthene, silica-mineral, ilmenite, and chromite with subordinate amounts of Fe-Ni metal and whitlockite. Hypersthene occurs as small euhedral grains in a fine-grained aggregate (Fig. 5), and includes a fine-grained silica-mineral. Pigeonitic pyroxene grains near the fine-grained aggregates often show a mosaic texture which appears to have formed by a mechanical process from a single phenocryst of pigeonitic pyroxene. The fine-grained aggregates seem to have been formed as intensely-shocked pockets by impact followed by recrystallization, because they show a continuous spectrum from a shock-darkened pockets to a highly-recrystallized pockets.

Table 2. Modal and bulk compositions of eucritic enclaves.

Enclave	Il-bearing enclaves							Il-free enclaves				
	Z	914	4631	(4627)	U	4632	Average	4630	4633	891	H	Average
Modes (vol%)												
Pl	38.1	39.4	41.9	40.4	34.7	44.1	39.8	44.3	47.6	47.0	46.7	46.4
Pig+Hyp	34.5	39.0	41.6	44.1	29.7	42.6	38.6	32.1	39.4	35.2	40.4	36.8
Aug	17.8	12.4	11.3	12.8	21.0	8.7	14.0	11.9	9.9	9.2	2.4	8.3
Silica	4.8	6.2	4.2	1.1	10.4	3.2	5.0	8.0	1.6	5.2	6.8	5.4
Fe-Phases	4.7	2.9	1.1	1.7	4.0	1.3	2.6	3.5	1.4	3.0	3.6	2.9
Phosphates	0.1	0.1	0.0	0.0	0.2	0.1	0.1	0.2	0.1	0.4	0.1	0.2
Total	100.0	100.0	100.0	100.0	100.0	100.0	100.0	100.0	100.0	100.0	100.0	100.0
Bulk compositions (wt%)												
SiO ₂	46.68	47.99	48.75	47.58	48.78	48.38	48.03	48.30	47.76	47.67	48.26	48.00
TiO ₂	0.22	0.25	0.34	0.23	0.27	0.32	0.27	0.10	0.05	0.11	0.00	0.07
Al ₂ O ₃	11.30	11.90	12.72	11.84	10.68	13.33	11.96	13.70	14.91	14.58	14.87	14.51
Cr ₂ O ₃	0.18	0.15	0.12	0.12	0.08	0.11	0.13	0.20	0.20	0.07	0.18	0.16
FeO	17.59	18.71	18.68	19.42	16.40	16.94	17.96	14.00	14.62	13.60	11.38	13.40
MnO	0.64	0.53	0.66	0.65	0.52	0.65	0.61	0.60	0.52	0.50	0.57	0.55
MgO	6.44	6.58	6.98	7.42	6.56	8.13	7.02	7.00	8.71	8.23	10.27	8.55
CaO	9.73	9.22	9.75	9.98	10.42	9.92	9.84	10.20	10.77	10.16	8.95	10.02
Na ₂ O	0.51	0.42	0.44	0.44	0.34	0.32	0.41	0.36	0.36	0.35	0.22	0.32
K ₂ O	0.02	0.02	0.03	0.02	0.01	0.02	0.02	0.02	0.04	0.00	0.01	0.02
Subtotal	93.31	95.77	98.47	97.70	94.06	98.12	96.24	94.48	97.94	95.27	94.71	95.60
mg	0.39	0.39	0.40	0.41	0.42	0.46	0.41	0.47	0.51	0.52	0.62	0.53
Rest	6.69	4.23	1.53	2.30	5.94	1.88	3.76	5.52	2.06	4.73	5.29	4.40
Fe from Rest	3.34	2.12	0.77	1.15	2.97	0.94	1.88	2.76	1.03	2.37	2.65	2.20
Fe from FeO	13.67	14.54	14.52	15.10	12.75	13.17	13.96	10.88	11.36	10.57	8.85	10.42
Total Fe	17.02	16.66	15.29	16.25	15.72	14.11	15.84	13.64	12.39	12.94	11.49	12.62

Modal phases are plagioclase (Pl), low-Ca pyroxene (Pigeonite+Hypersthene), high-Ca pyroxene (Aug), silica-mineral (Silica), Fe-phases (such as troilite, Fe-Ni metal and the altered products, chromite, and ilmenite), and phosphates. The major element compositions of each sample were calculated using the modal compositions of the silicates and their assumed densities. The "Rest" (100 wt%—subtotal for the bulk composition) is ascribed mainly to the Fe-phases, and "Fe from Rest" is Fe wt% obtained by assuming 50% Fe content of the "Rest".

Table 3. Mineral assemblages of the eucritic enclaves.

	Il-bearing group						Il-free group			
	Z	914	4631	4627	U	4632	4630	4633	891	H
Major components										
Cpx	+	+	+	+	+	+	+	+	+	+
(mg)	30-35	36-38	37-40	39-41	38-42	44-47	43-50	48-51	49-52	60-64
Pl	+	+	+	+	+	+	+	+	+	+
(An)	82-91	88-91	88-91	88-92	88-91	89-94	91-93	90-94	90-94	95-98
Sil	+	+	+	+	+	+	+	+	+	+
Minor components										
Opx	+						+	+	+	+
(mg)	52-54						50-55	52-62	53-57	64-66
Ol	+									
(mg)	13-17									
Zir	+									
Chm	+	+	+	+	+	+	+	+	+	+
(2Ti)	13-27	12-29	12-26	23-31	15-26	10-25	8-17	3-4	9-14	0-3
Il	+	+	+	+	+	+				
Rut		+				+				
Whit	+	+	+		+	+	+	+	+	+
F-ap		+		+	+					
Metal	+	+	+	+	+	+	+	+	+	+
Tr	+	+	+	+	+	+	+	+	+	+

Cpx, Pl, Sil, Opx, Ol, Zir, Chm, Il, Rut, Whit, F-ap, Metal, and Tr are clinopyroxene, plagioclase, silica-mineral, orthopyroxene, olivine, zircon, chromite, ilmenite, rutile, whitlockite, fluorapatite, Fe-Ni metal, and troilite, respectively. The *mg* and *An* are MgO/(MgO+FeO) and Ca/(Ca+Na+K) molecular %, respectively. The 2Ti for chromite is 2Ti/(Al+Cr+2Ti) which means the molecular % of ulvöspinel.

3.2. Enclave 914 from Vaca Muerta (*mg*=0.39, *Il*-bearing)

Enclave 914 has a coarse-grained gabbroic texture (Fig. 6), and a preferred orientation due to a weak parallelism of the long axes of pigeonite grains. Large pigeonites often include irregular smaller pigeonite grains which have different extinction angles from the host pigeonite. Chromite occurs as large grains which often include very thin exsolution lamellae of ilmenite (Fig. 7). Besides as lamellae in chromite, primary ilmenite occurs as isolated large grains or as intergrowths with rutile. Rutile always occurs as an intergrowth with ilmenite (Fig. 8), and the volume of rutile and ilmenite in the intergrowth seems to be nearly equal. The common phosphate is whitlockite, and fluorapatite is rare.

3.3. Enclave 4631 from Vaca Muerta (*mg*=0.40, *Il*-bearing)

This has a medium-grained porphyritic to gabbroic texture (Fig. 9). Pigeonite shows weak exsolution lamellae (narrower than a few microns). A silica-mineral (mostly tridymite) occurs as small or large grains often surrounded by clinopyroxene (Fig. 9).

3.4. Sample 4627 found in northern Chile (*mg*=0.41, *Il*-bearing)

This has a coarse-grained gabbroic texture (Fig. 10). Pyroxene shows thin ex-



Fig. 1. Enclave Z, showing a subophitic texture consisting of plagioclase (Pl) and pigeonitic pyroxene (Pg). Transmitted light, open Nicols, and width of 2 mm.

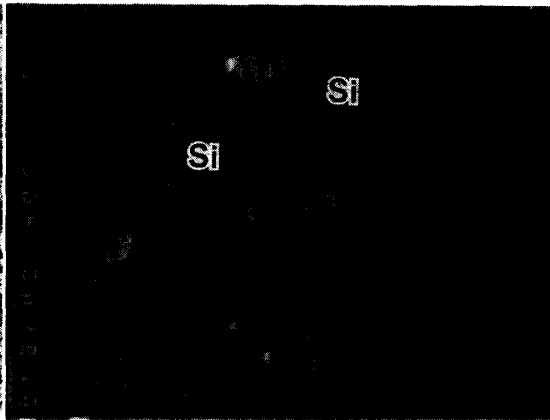


Fig. 2. Enclave Z. Backscattered electron (BSE) image showing olivine (Ol) and silica-mineral (Si) inclusions in pigeonite (Pg), with exsolution lamellae. Width of 62 microns.

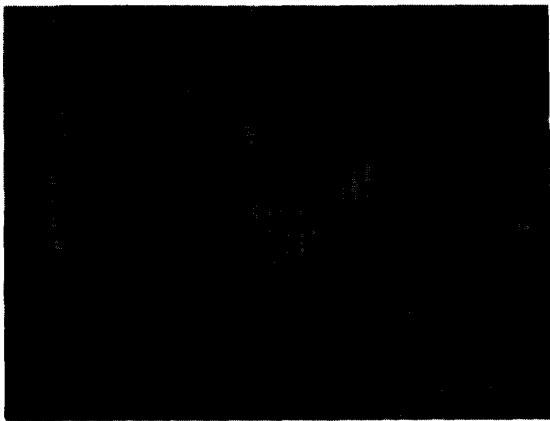


Fig. 3. Enclave Z. BSE image showing zircon (Zr) partially included in ilmenite (Il). Black portions are silicates. Width of 94 microns.

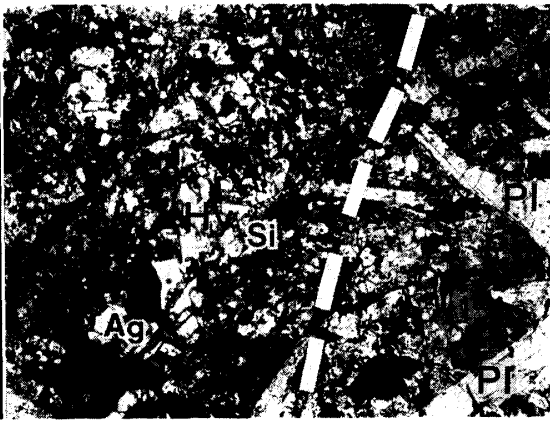


Fig. 4. Enclave Z. Left of the white line are fine-grained aggregates consisting mainly of hypersthene (Hy), augite (Ag), tridymite (Si), troilite, and altered Fe-Ni metal. Transmitted light, open Nicols, and width of 2 mm.



Fig. 5. Enclave Z. BSE image showing the central portion of Fig. 4. Tr and aM are troilite and altered Fe-Ni metal, respectively. Width of 660 microns.



Fig. 6. Enclave 914, showing coarse-grained gabbroic texture. Transmitted light, open Nicols, and width of 2 mm.

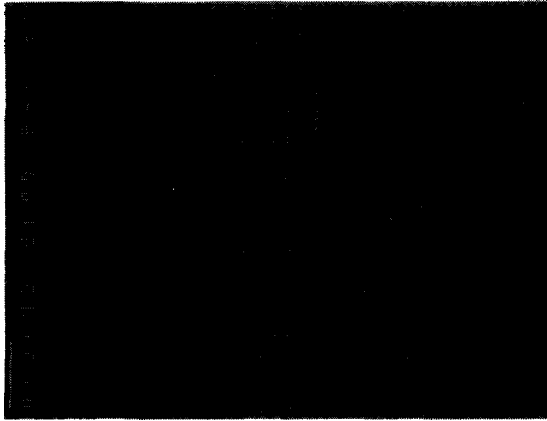


Fig. 7. Enclave 914. BSE image showing very thin exsolution lamellae of ilmenite in a large chromite grain. Width of 85 microns.



Fig. 8. Enclave 914. BSE image showing intergrowth of ilmenite (Il) and rutile (Rt). A small chromite (Cm) grain occurs in the right portion of the intergrowth. Width of 610 microns.

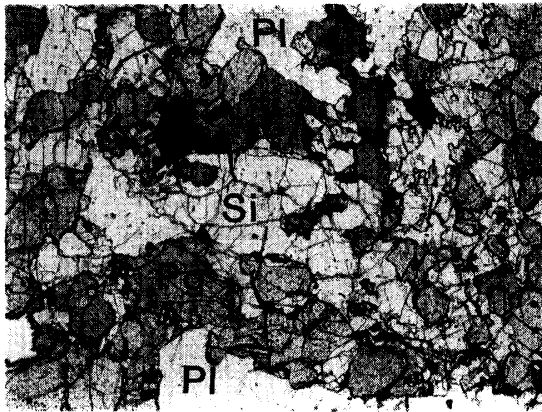


Fig. 9. Enclave 4631, showing medium-grained gabbroic to granular texture. Transmitted light, open Nicols, and width of 2 mm.

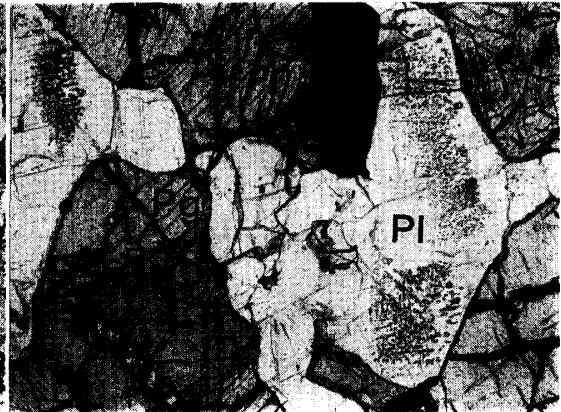


Fig. 10. Euclitic sample 4627, showing coarse-grained gabbroic texture. Transmitted light, open Nicols, and width of 2 mm.

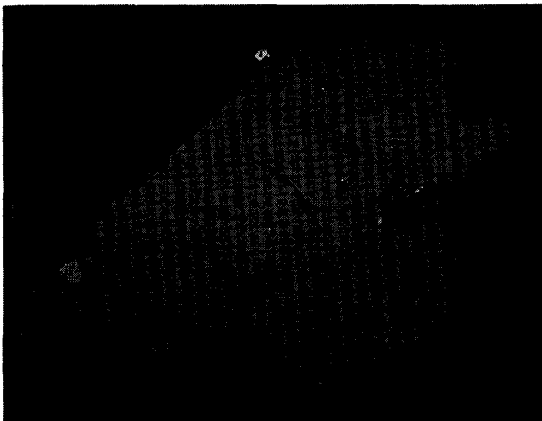


Fig. 11. Euclitic sample 4627. BSE image showing intergrowth of ilmenite (Il) and chromite (Cm). Width of 250 microns.

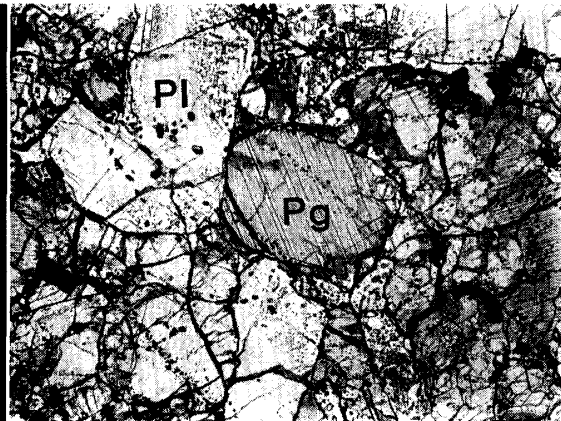


Fig. 12. Enclave U, showing medium to coarse-grained subophitic texture. Transmitted light, open Nicols, and width of 2 mm.

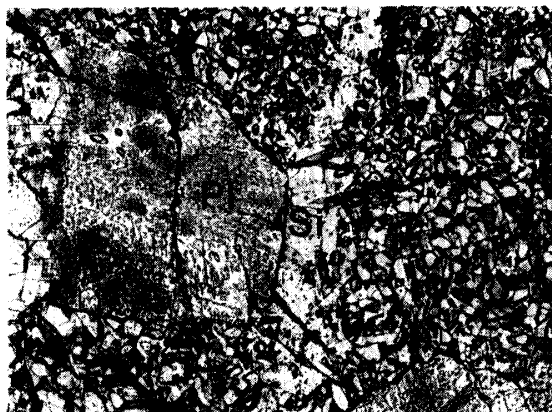


Fig. 13. Enclave U. Fine-grained aggregate consisting mainly of augite and tridymite. Large phenocrystic plagioclase (Pl) is cloudy with tiny augitic grains, and long needles of tridymite (Si). Transmitted light, open Nicols, and width of 2 mm.

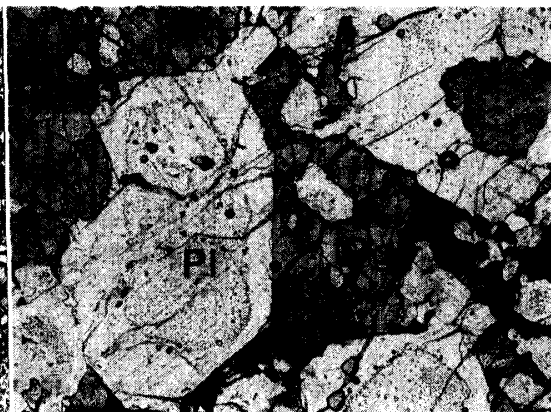


Fig. 14. Enclave 4632, showing medium-grained subophitic texture with phenocrystic cloudy plagioclase (Pl). Transmitted light, open Nicols, and width of 2 mm.

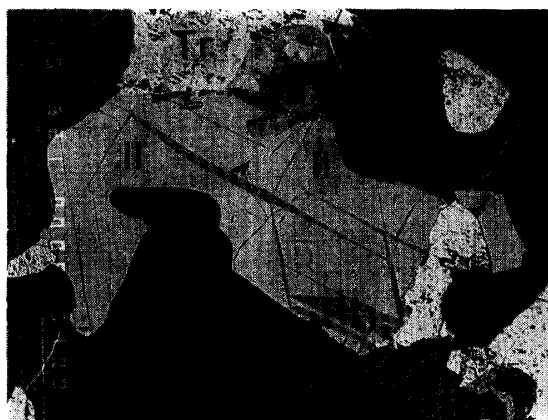


Fig. 15. Enclave 4632. BSE image showing intergrowth of ilmenite (Il) and rutile (Rt). Width of 340 microns.

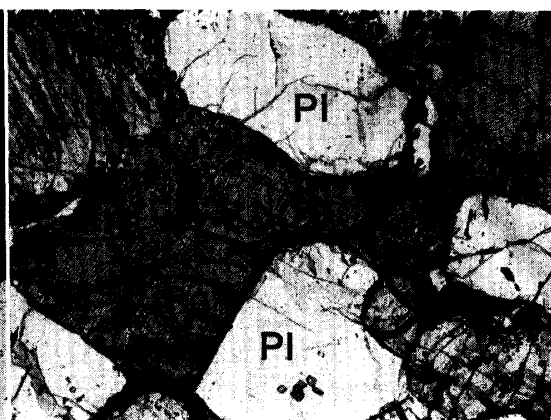


Fig. 16. Enclave 4630, showing coarse-grained gabbroic to granular texture. Transmitted light, open Nicols, and width of 2 mm.



Fig. 17. Enclave 4633, showing coarse-grained gabbroic to granular texture. Transmitted light, open Nicols, and width of 2 mm.



Fig. 18. Enclave 4633, showing euhedral tridymite (Si) in plagioclase (Pl) and pigeonite (Pg). Transmitted light, open Nicols, and width of 2 mm.

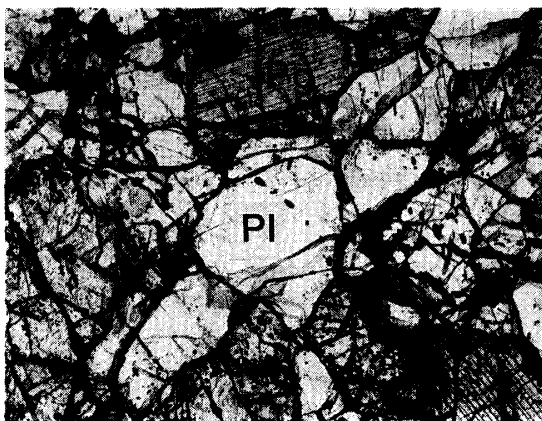


Fig. 19. Enclave 891, showing coarse-grained gabbroic to granular texture. Transmitted light, open Nicols, and width of 2 mm.

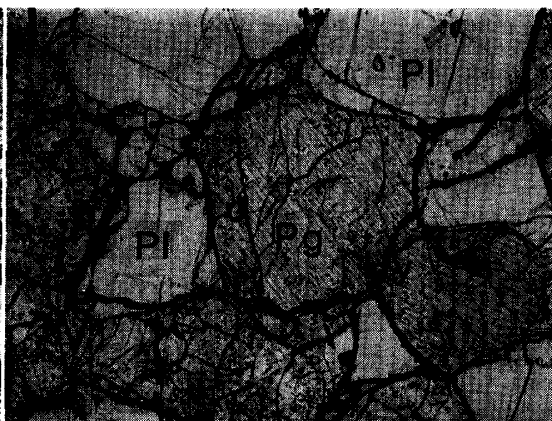


Fig. 20. Enclave H, showing coarse-grained granular texture. Transmitted light, open Nicols, width of 2 mm.



Fig. 21. Enclave H, the same as Fig. 20. Pigeonitic pyroxene (Pg) is replaced by hypersthene (Hy). Transmitted light, cross Nicols, and width of 2 mm.

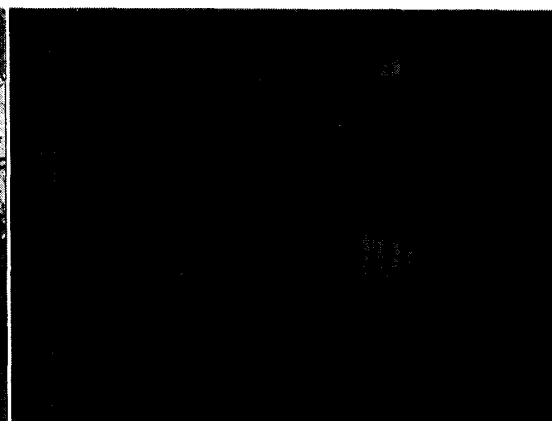


Fig. 22. Enclave H. BSE image showing troilite (Tr) and silica-mineral (Si) inclusions in hypersthene (Hy). Width of 50 microns.

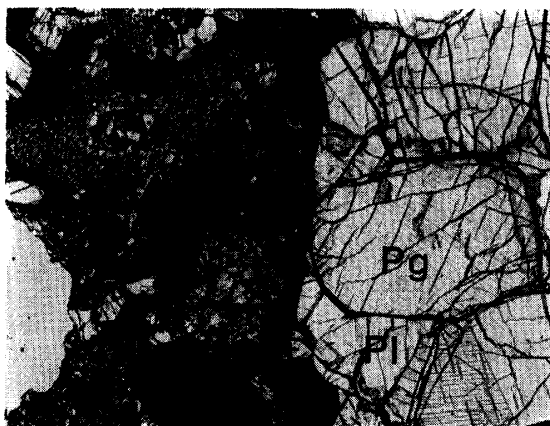


Fig. 23. Enclave H, showing the boundary with the host mesosiderite (Mt. Padbury). Note that a pigeonite grain in direct contact with the host mesosiderite is not replaced by hypersthene. Transmitted light, open Nicols, and width of 2 mm.

solution lamellae. A small amount of augite occurs as isolated grains. Phenocrysts of plagioclase often include tiny pyroxene grains, and these tiny grains are distributed parallel to the euhedral form of plagioclase (Fig. 10). The silica-mineral is rare. Chromite and ilmenite occur as isolated grains or as intergrowths (Fig. 11).

3.5. *Enclave U from Mt. Padbury (mg=0.42, Il-bearing)*

This has a medium- to coarse-grained subophitic to porphyritic texture (Fig. 12). Pigeonite shows moderate exsolution lamellae (a few microns wide). Plagioclase often occurs as euhedral phenocrysts. The silica-mineral (mostly tridymite) occurs as large long needles up to 2 mm in length and 0.1 to 0.2 mm in width. Phosphate is mainly whitlockite, and fluorapatite is rare. This enclave includes fine-grained aggregates (Fig. 13), which consist mainly of augite and silica-mineral. Plagioclase in contact with the fine-grained aggregates is dusted with very tiny inclusions, smaller than several microns, of augitic pyroxene, and these tiny inclusions are less common in plagioclase far from the fine-grained aggregates. The fine-grained aggregates may have been formed as mesostasis or as shock-melt pockets followed by recrystallization.

3.6. *Enclave 4632 from Vaca Muerta (mg=0.46, Il-bearing)*

Enclave 4632 has a medium-grained subophitic to porphyritic texture (Fig. 14). Pigeonite shows thin exsolution lamellae, and contains many inclusions of plagioclase and irregular pyroxene. Plagioclase often occurs as large phenocrysts, which become dusty with many tiny inclusions in the central portion. Silica-minerals occur as microphenocrysts or interstitial grains. Rutile occurs as lamellae in ilmenite (Fig. 15), and the volume of rutile is always less than that of the host ilmenite.

3.7. *Enclave 4630 from Vaca Muerta (mg=0.47, Il-free)*

This is coarse-grained and has a gabbroic to granular texture (Fig. 16). Pigeonite shows moderate exsolution lamellae (a few to ten microns in width). Augite occurs as isolated grains in a small amount. The peripheral portions of clinopyroxenes are partly modified to an aggregate of hypersthene and finer troilite. Silica-minerals occur as large grains up to 2 mm across and sometimes include plagioclase or pyroxene grains.

3.8. *Enclave 4633 from Vaca Muerta (mg=0.51, Il-free)*

This has a coarse-grained equigranular texture (Fig. 17). Pigeonite occurs as irregular or rounded grains showing moderate exsolution lamellae (a few to ten microns in width). Augite occurs as isolated grains. Plagioclase is subhedral or rounded grains, and the triple junctions of plagioclase and/or pigeonite grains sometimes have angles of near 120°. Silica-minerals occur as interstitial grains and rarely show a euhedral form; they are included partly in pyroxene and partly in plagioclase (Fig. 18).

3.9. *Enclave 891 from Vaca Muerta (mg=0.52, Il-free)*

This has a coarse-grained gabbroic to granular texture (Fig. 19). The degree of

exsolution lamellae of augite is moderate (a few to ten microns in width) in pigeonite. Pigeonite sometimes shows textural evidence of being replaced by hypersthene in the peripheral portions of the grains.

3.10. Enclave H from Mt. Padbury ($mg=0.62$, Il-free)

This has a coarse-grained equigranular texture (Fig. 20). Pigeonite had more or less suffered replacement (see Discussion in Section 5.2) by hypersthene which includes tiny troilite and silica-mineral grains (Fig. 21). Plagioclase and pyroxene occur as granular grains, and the triple junctions of these grains often show angles of near 120°C . Silica-minerals (mostly tridymite) occur as large grains comparable to plagioclase or pyroxene grains.

4. Mineralogy

Representative chemical compositions of silicates and oxides in each sample are shown in Table 4.

4.1. Pyroxene

The predominant pyroxene in all samples is pigeonite and, as shown in Fig. 24, most pigeonites have homogeneous mg values. This suggests that the original igneous MgO-FeO zoning has mostly been erased.

Augite occurs as lamellae in pigeonite in all samples. The thinness of these lamellae results in a continuous spectrum of chemical composition, from pigeonite to augite (Fig. 24). This is due to the overlap of both phases during EPMA analyses. Besides as lamellae in pigeonites, augite occurs as isolated grains in eucritic sample 4627 and enclaves 4630, 4633, and 891. In enclaves Z and U, augite occurs as small grains in the fine-grained aggregates. A phenocryst of clinopyroxene in enclave Z, in direct contact with a fine-grained aggregate, shows reverse MgO-FeO zoning, from ferroan pigeonitic core to magnesian augitic rim (Fig. 24).

Orthopyroxene (hypersthene) occurs in the peripheral portions of pigeonites in the Il-free enclaves 4630, 4633, 891, and H, indicating that they are replacement textures. They are always more magnesian than the pigeonite (Fig. 24). Hypersthene in a fine-grained aggregate in enclave Z is discontinuously magnesian in comparison with coexisting pigeonite. It seems to be in equilibrium with magnesian augite which occurs in the fine-grained aggregates.

4.2. Olivine

Ferroan olivine with mg values of 0.13 to 0.17 occurs in enclave Z. The mg values are within the range of ferroan olivines found in HED meteorites (DESNOYERS, 1982). The ferroan olivine in enclave Z may be a product of the latest-stage of magmatic crystallization. However, it always occurs as small inclusions in pigeonite and not as isolated grains between grain boundaries. Another explanation for the olivine occurrence is that a small amount of ferroan pigeonite crystallized from magma, metastably, in the forbidden zone of the pyroxene quadrilateral (LINDSLEY and

Table 4. Representative compositions (wt %) of the silicates and oxides in the eucritic enclaves.

The minerals are: plagioclase (Pl), pigeonite (Pig), augite (Aug), hypersthene (Hyp), chromite (Chm), ilmenite (Il), olivine (Ol), and rutile (Rut).

	Enclave Z (Il-bearing)								Enclave 914 (Il-bearing)					
	Pl	Pig	Aug	Hyp	Chm	Chm	Il	Ol	Pl	Pig	Aug	Chm	Il	Rut
SiO ₂	46.31	47.36	51.05	50.28	0.00	0.04	0.02	30.75	44.85	48.49	49.77	0.00	0.00	0.00
TiO ₂	0.00	0.24	0.68	0.30	8.84	3.32	52.54	0.03	0.00	0.35	0.68	10.46	54.33	100.26
Al ₂ O ₃	34.03	0.42	0.89	0.43	6.14	8.50	0.00	0.00	34.17	0.33	1.27	5.89	0.02	0.00
Cr ₂ O ₃	0.00	0.23	0.48	0.28	43.02	51.67	0.07	0.12	0.00	0.20	0.44	41.60	0.06	0.00
FeO	0.41	38.28	12.78	27.55	39.39	32.02	45.79	59.59	0.13	36.07	19.14	39.13	40.70	0.08
MnO	0.00	1.35	0.57	1.18	1.10	1.41	0.91	1.51	0.00	1.04	0.52	1.28	2.14	0.00
MgO	0.03	10.07	13.00	17.33	0.55	2.17	0.58	6.40	0.03	11.60	10.40	1.24	1.73	0.00
CaO	17.38	0.94	19.74	1.59	0.21	0.00	0.00	0.19	18.71	1.10	18.00	0.00	0.02	0.02
Na ₂ O	1.53	0.00	0.08	0.07	0.00	0.00	0.00	0.05	1.20	0.00	0.10	0.00	0.00	0.00
K ₂ O	0.07	0.04	0.00	0.00	0.00	0.00	0.00	0.00	0.05	0.00	0.00	0.00	0.00	0.00
Total	99.76	98.93	99.27	99.01	99.25	99.13	99.91	98.64	99.14	99.18	100.32	99.60	99.00	100.36

	Enclave 4631 (Il-bearing)					AMNH 4627 (Il-bearing)					Enclave U (Il-bearing)				
	Pl	Pig	Aug	Chm	Il	Pl	Pig	Aug	Chm	Il	Pl	Pig	Aug	Chm	Il
SiO ₂	44.82	48.87	50.39	0.00	0.00	44.30	48.92	49.27	0.00	0.00	44.55	48.79	49.03	0.00	0.00
TiO ₂	0.10	0.44	0.74	5.82	52.68	0.08	0.21	0.69	9.34	53.69	0.00	0.33	0.71	8.76	53.69
Al ₂ O ₃	34.22	0.38	0.97	7.54	0.04	34.42	0.23	0.82	6.38	0.00	34.73	0.25	0.84	6.50	0.00
Cr ₂ O ₃	0.00	0.16	0.30	47.92	0.15	0.00	0.13	0.37	42.03	0.09	0.00	0.07	0.23	43.41	0.06
FeO	0.20	34.71	17.09	36.52	44.26	0.16	34.44	18.18	39.29	44.54	0.12	35.82	18.24	38.61	45.19
MnO	0.09	1.24	0.50	0.56	0.91	0.00	1.14	0.68	0.67	0.85	0.00	1.10	0.64	0.44	0.95
MgO	0.05	11.97	10.33	0.73	0.94	0.00	12.30	10.16	1.00	1.34	0.05	12.29	10.33	0.84	1.01
CaO	18.09	1.83	18.81	0.00	0.05	18.27	2.49	19.09	0.00	0.00	18.79	1.29	18.98	0.00	0.00
Na ₂ O	1.13	0.00	0.05	0.00	0.00	1.23	0.00	0.13	0.00	0.00	1.10	0.00	0.06	0.00	0.00
K ₂ O	0.09	0.00	0.00	0.00	0.00	0.05	0.00	0.00	0.00	0.00	0.04	0.00	0.00	0.00	0.00
Total	98.79	99.60	99.18	99.09	99.03	98.51	99.86	99.39	98.71	100.51	99.38	99.94	99.06	98.56	100.90

Enclaves in the Mesosiderites

Table 4. (continued).

	Enclave 4632 (Il-bearing)						Enclave 4630 (Il-free)					Enclave 4633 (Il-free)		
	Pl	Pig	Aug	Chm	Il	Rut	Pl	Pig	Aug	Hyp	Chm	Pl	Pig	Aug
SiO ₂	43.93	48.79	49.81	0.00	0.00	0.03	44.75	49.75	51.84	51.09	0.00	43.99	50.45	50.95
TiO ₂	0.00	0.51	0.72	5.36	53.75	98.40	0.05	0.25	0.29	0.26	3.84	0.00	0.08	0.12
Al ₂ O ₃	34.63	0.38	1.50	8.30	0.00	0.00	34.74	0.30	0.51	0.29	8.70	35.49	0.57	0.84
Cr ₂ O ₃	0.00	0.12	0.55	49.50	0.00	0.16	0.00	0.18	0.32	0.17	52.27	0.00	0.30	0.52
FeO	0.00	32.32	13.63	33.53	43.23	0.67	0.07	30.38	13.35	27.82	33.35	0.18	28.68	13.25
MnO	0.00	1.24	0.50	0.89	1.37	0.00	0.00	1.18	0.55	1.09	1.00	0.00	1.03	0.42
MgO	0.04	14.31	12.47	1.08	1.99	0.03	0.03	15.93	13.02	17.43	1.11	0.06	16.09	12.20
CaO	19.09	2.00	18.62	0.00	0.00	0.00	18.71	1.37	20.18	1.43	0.03	19.20	1.54	20.23
Na ₂ O	0.85	0.05	0.11	0.00	0.00	0.00	0.89	0.00	0.10	0.00	0.00	0.80	0.05	0.12
K ₂ O	0.04	0.00	0.00	0.00	0.00	0.00	0.02	0.00	0.00	0.00	0.00	0.00	0.00	0.00
Total	98.58	99.72	97.91	98.66	100.34	99.29	99.26	99.34	100.16	99.58	100.30	99.72	98.79	98.65

	Enclave 4633 (Il-free)		Enclave 891 (Il-free)			Enclave H (Il-free)							
	Hyp	Chm	Pl	Pig	Aug	Hyp	Chm	Pl	Pig	Aug	Hyp	Chm	Chm
SiO ₂	50.06	0.00	44.21	50.68	51.17	50.69	0.00	43.12	51.74	52.48	52.10	0.00	0.00
TiO ₂	0.21	1.29	0.00	0.20	0.27	0.17	4.10	0.00	0.00	0.09	0.04	0.00	0.91
Al ₂ O ₃	0.39	10.25	34.96	0.25	0.59	0.37	8.05	36.09	0.32	0.59	0.49	11.32	10.26
Cr ₂ O ₃	0.38	54.74	0.00	0.07	0.37	0.19	51.16	0.00	0.36	0.55	0.46	55.25	54.89
FeO	24.16	32.13	0.21	30.35	12.63	26.60	33.97	0.08	23.55	11.03	21.25	28.63	29.87
MnO	1.05	0.66	0.00	1.08	0.62	0.88	1.10	0.00	1.17	0.77	1.27	0.76	1.05
MgO	21.11	1.53	0.03	16.98	13.62	18.76	1.00	0.02	20.96	16.13	21.83	2.99	2.11
CaO	1.38	0.00	18.48	1.22	20.32	1.40	0.03	19.48	1.18	17.52	1.31	0.00	0.00
Na ₂ O	0.03	0.00	0.83	0.00	0.05	0.00	0.02	0.43	0.08	0.12	0.03	0.00	0.00
K ₂ O	0.00	0.00	0.00	0.00	0.00	0.00	0.00	0.03	0.00	0.03	0.00	0.00	0.00
Total	98.77	100.60	98.72	100.83	99.64	99.06	99.43	99.25	99.36	99.31	98.78	98.95	99.09

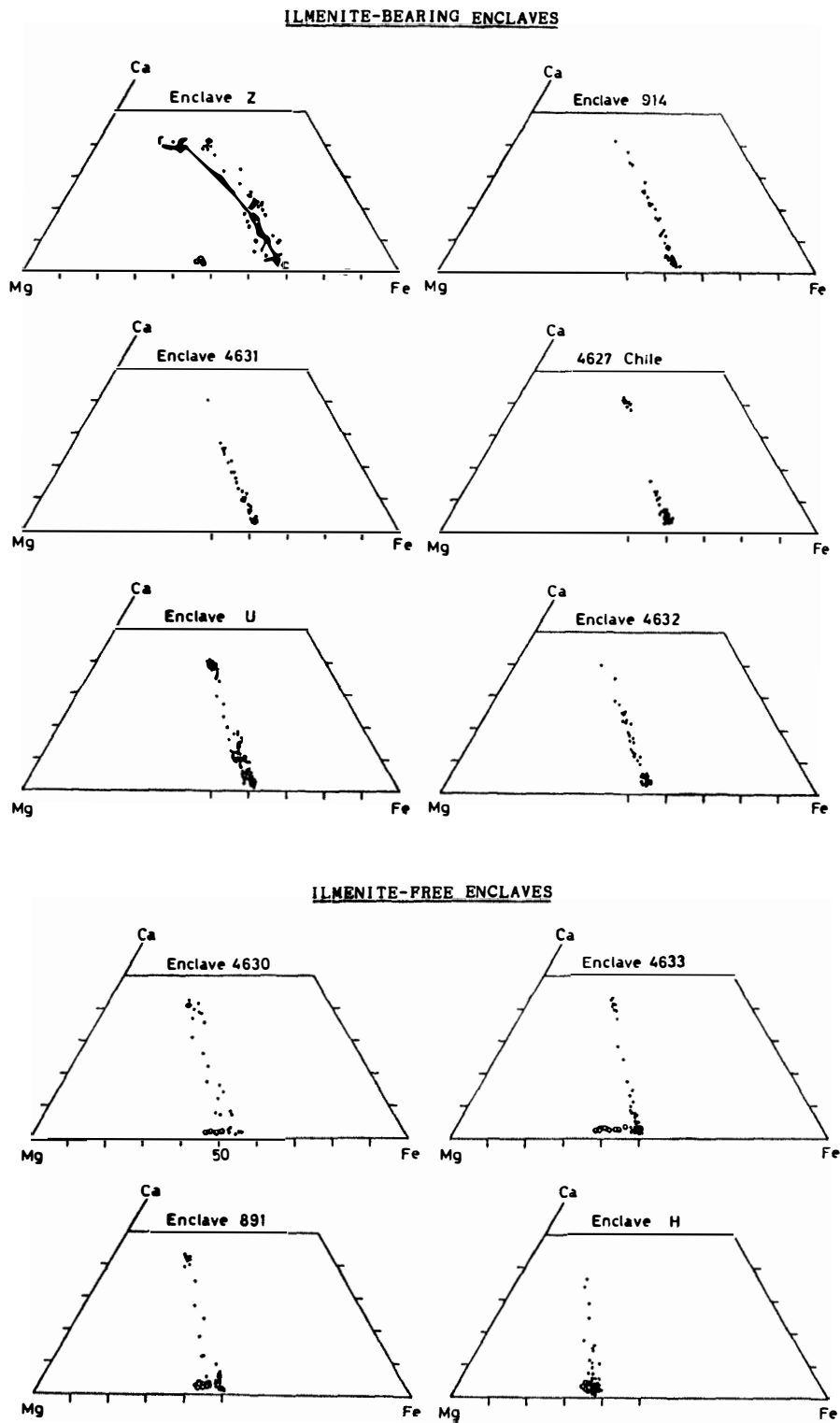


Fig. 24. Ca-Mg-Fe atomic ratios of clinopyroxene (solid circle), orthopyroxene (open circle), and olivine (solid square) in nine enclaves from mesosiderites and one eucritic sample from Chile. In the quadrilateral for enclave Z, chemical zoning from core (c) to rim (r) in a clinopyroxene grain which contacts directly with a fine-grained aggregate is shown by a solid line. Note that Il-bearing enclaves are more Fe-rich than Il-free enclaves.

ANDERSEN, 1982). It then decomposed into ferroan olivine and a silica-mineral, under subsolidus conditions; the silica-mineral occurs near the olivine as shown in Fig. 2.

4.3. *Plagioclase*

Plagioclase is the predominant phase in all of the samples. It is homogeneous in chemical composition or shows slight normal zoning from a calcic core to a sodic rim. The compositional range of plagioclase in each sample is shown in Table 3. Most plagioclase in the Il-bearing group is more sodic (An_{82-94}) than that in the Il-free group (An_{91-98}). Plagioclase in enclave H is extremely calcic, with a range of An_{95-98} , whereas a small plagioclase grain included in the rim of a large, zoned, chromite grain is more sodic, with An_{89-91} .

4.4. *Silica-mineral*

A silica-mineral occurs in all of the samples studied, and is mostly tridymite. In some enclaves it occurs as phenocrysts or microphenocrysts, and in some enclaves as small rounded grains included in plagioclase or pyroxene. In the fine-grained aggregates in enclaves Z and U, the silica-minerals occur as a major phase.

4.5. *Chromite*

Chromite occurs in all samples studied. Chromites in the enclaves are very similar in compositional trend to those in the howardites (Fig. 25). Chromites in the enclaves are homogeneous within grains, but vary between grains. However, chromite in enclave H shows a slight normal zoning from a TiO_2 -poor core to a TiO_2 -rich rim.

Generally, chromites in the more ferroan enclaves are richer in TiO_2 (ulvospinel component). However, chromites in enclave Z show a bimodal distribution in chemical composition. The TiO_2 -poor chromites (solid circles in Fig. 25) occur in the fine-grained aggregates, and seem to be non-magmatic, whereas the TiO_2 -rich chromites are magmatic.

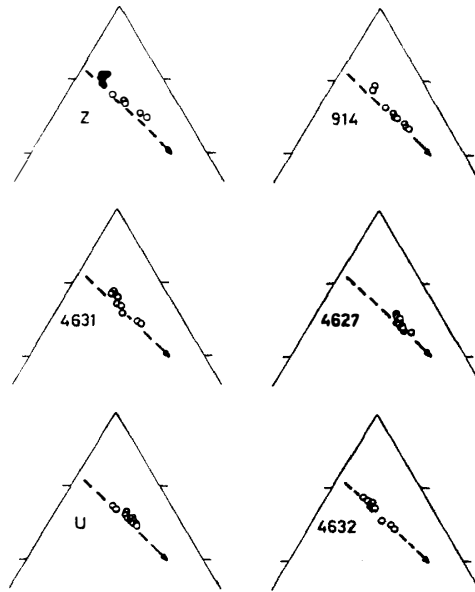
Chromite in enclave 914 includes thin lamellae of ilmenite with three orientations (Fig. 7) which probably correspond to (1 1 1) of the host chromite. The lamellae are due to exsolution from chromite solid solution.

4.6. *Ilmenite and rutile*

Ilmenite grains occur in samples with mg values smaller than 0.46, and do not occur in samples with mg values larger than 0.47. Generally, ilmenite/chromite volume ratios seem to increase in the more ferroan samples. This tendency is the same as that in eucritic clasts in howardites.

Rutile occurs as intergrowths with ilmenites in two enclaves, 914 and 4632, and the volumes of rutile and ilmenite in enclave 914 are nearly equal (Fig. 8). This suggests that the intergrowth was originally ferropseudobrookite or armalcolite. Ferropseudobrookite decomposes at $1140^\circ C$ into the assemblage rutile and ilmenite (LINDSLEY, 1965). On the other hand, the volume ratio of rutile to ilmenite in enclave 4632 is far smaller than 1 (Fig. 15), suggesting that the rutile lamellae may be due to

ILMENITE-BEARING ENCLAVES



ILMENITE-FREE ENCLAVES

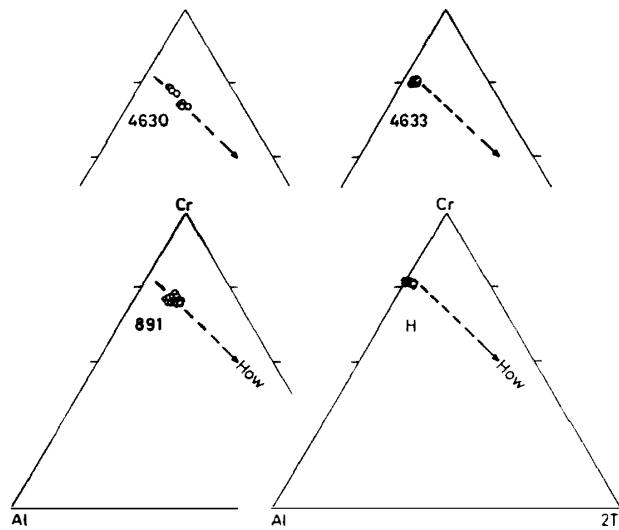


Fig. 25. Cr-Al-2Ti atomic ratios of chromite solid solutions, showing the molecular ratios of chromite, Al-spinel, and ulvospinel. In the triangle for enclave Z, solid circles are chromites which occur in fine-grained aggregates. Dashed arrow (How) is the chemical trend for chromites in the Y-7308 howardite (IKEDA and TAKEDA, 1985). Note that chromites in Il-free enclaves are poorer in Ti than those in Il-bearing enclaves.

exsolution from ilmenite solid solution.

4.7. Zircon

Only one zircon grain was found and it occurs in enclave Z from Mt. Padbury (Fig. 3). The composition of the grain is: SiO₂=32.9 wt%, ZrO₂=65.8 wt%, and

Table 5. Chemical compositions (wt%) of the phosphates (whitlockite and fluorapatite) and Ca-Fe-P phases (CFP) in the eucritic enclaves.

Il-bearing enclaves											
	Enclave Z		Enclave 914			Enclave 4631		AMNH 4627		Enclave U	
	Whitl	Whitl	Whitl	F-Ap	CFP	Whitl	CFP	F-Ap	F-Ap	Whitl	F-Ap
FeO	0.98	0.26	1.52	0.80	3.36	2.64	54.68	0.71	0.51	0.70	0.25
MnO	0.38	0.34	0.21	0.00	0.39	0.00	0.00	0.00	0.00	0.00	0.00
MgO	3.31	3.59	3.05	0.04	2.36	2.75	0.19	0.03	0.00	3.63	0.00
CaO	46.11	46.60	46.30	54.06	41.18	43.72	0.88	55.52	53.25	45.87	52.81
Na ₂ O	1.01	1.18	0.99	0.00	0.48	0.85	0.42	0.00	0.00	1.20	0.00
P ₂ O ₅	46.97	47.25	46.01	41.04	40.56	46.74	38.73	41.14	42.58	47.21	43.51
Y ₂ O ₃	0.29	0.21	0.26	0.00	0.88	1.12	1.11	0.03	0.04	0.53	0.02
Ce ₂ O ₃	0.13	0.07	0.09	0.00	0.29	0.51	1.05	0.03	0.01	0.41	0.05
F				3.74		0.07	0.09	1.37	2.21	0.56	3.12
Cl				0.67		0.02	0.03	0.19	0.00	0.00	0.12
Total	99.18	99.50	98.43	100.35	89.50	98.42	97.18	99.02	98.60	100.11	99.88

Il-bearing enclaves				Il-free enclaves								
Enclave U		Enclave 4632		Enclave 4630		Enclave 4633		Enclave 891		Enclave H		
CFP	CFP	Whitl	CFP	Whitl	Whitl	Whitl	Whitl	Whitl	Whitl	Whitl	Whitl	
FeO	9.91	30.88	1.42	3.15	1.66	1.75	0.76	0.60	0.97	1.04	0.77	0.74
MnO	0.00	0.14	0.22	0.23	0.00	0.13	0.00	0.19	0.26	0.33	0.30	0.36
MgO	1.38	0.56	2.98	2.37	3.18	3.10	3.77	3.75	3.27	3.19	3.62	3.28
CaO	30.69	11.57	44.75	40.19	47.82	47.64	46.68	47.99	46.47	45.51	46.47	46.70
Na ₂ O	0.33	0.18	1.00	0.87	0.97	0.85	0.97	0.89	0.93	1.05	1.06	0.74
P ₂ O ₅	35.92	31.78	47.08	43.03	46.52	46.20	47.39	45.96	47.09	47.92	47.72	47.97
Y ₂ O ₃	1.17	1.03	0.57	0.56	0.01	0.02	0.00	0.01	0.00	0.00	0.01	0.00
Ce ₂ O ₃	1.75	1.68	0.48	0.61	0.00	0.01	0.01	0.00	0.01	0.00	0.00	0.01
F	0.49	0.28	0.47	0.51								
Cl	0.01	0.03	0.03	0.00								
Total	81.65	78.13	99.00	91.52	100.16	99.70	99.58	99.39	99.00	99.04	99.95	99.80

$\text{HfO}_2 = 1.4 \text{ wt}\%$. Repeated analyses of HfO_2 are from 1.2 to 1.6 wt%, because of the small size of the zircon grain. The presence of zircon in the Vaca Muerta mesosiderite was reported by MARVIN and KLEIN (1964), and the existence of zircon in Mt. Padbury suggests that zircon might occur ubiquitously in mesosiderites, whereas it rarely occurs in HED meteorites.

4.8. Phosphates

Whitlockite is found in all of the samples studied, except for 4627; however, it may nevertheless occur. Fluorapatite occurs in 914, 4627, and U, but the amount is far less than the coexisting whitlockite. Chemical compositions of phosphates are shown in Table 5. Phosphates in 4631, U, and 4632 show a wide compositional range, from stoichiometric whitlockite to a non-stoichiometric Ca-, Fe-, and P-bearing phase (CFP phase, hereafter). The CFP phase seems to be produced from whitlockite by terrestrial alteration: the MgO and Na_2O contents decrease from stoichiometric whitlockite with increasing FeO; CaO and P_2O_5 also decrease. Total CaO, MgO, Na_2O , FeO, and P_2O_5 ranges from 80 to 95 wt% for the CFP phase. H_2O , OH, O, and/or CO_3 may be contained in the CFP phase.

The Y_2O_3 and Ce_2O_3 contents of whitlockite and the CFP phase in Il-bearing enclaves are plotted in Fig. 26. The Y_2O_3 and Ce_2O_3 contents of fluorapatite are very low in comparison with the coexisting whitlockite (Table 5) and not shown in Fig. 26. Whitlockites in enclaves Z and 914 have the same Ce/Y ratios as that of C1 (Orgueil) chondrites. However, whitlockites in enclaves 4631, U, and 4632 have Ce/Y ratios slightly larger than that in C1 chondrites. The CFP phases in enclaves 4631, U, and 4632 show a wide range of the Y_2O_3 and Ce_2O_3 contents which are different from those of whitlockites: the Ce/Y ratios of the CFP phases are larger than those of whitlockites. On the other hand, the Y_2O_3 and Ce_2O_3 contents of whitlockites in the Il-free enclaves

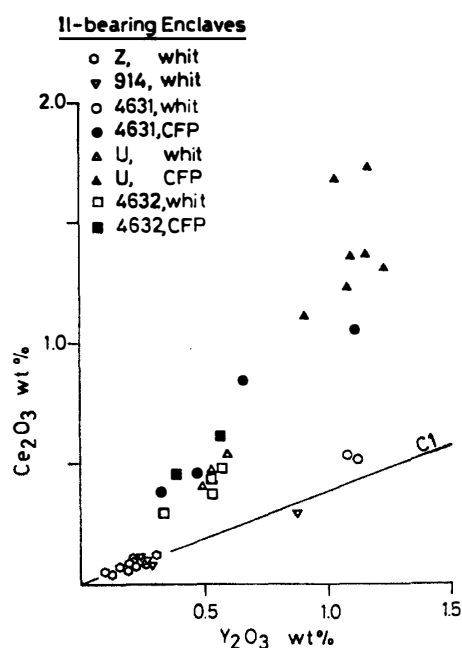


Fig. 26. Y_2O_3 and Ce_2O_3 (wt %) in whitlockites (open symbols) and Ca-Fe-P-bearing phases (CFP, solid symbols) in Il-bearing enclaves. The straight line labelled C1 shows the Ce/Y ratio of C1 chondrites (Orgueil: ANDERS and EBHARA, 1982). All whitlockites in Il-free enclaves (4630, 4633, 891, and H) are below the detection limit (0.025 wt% for Y_2O_3 , 0.05 wt% for Ce_2O_3).

Table 6. Chemical compositions of the Fe-Ni metal (Met) and troilite (Tr) in the eucritic enclaves.

II-bearing enclaves															
Enclave Z			Enclave 914			Enclave 4631			AMNH 4627			Enclave U			
	Met	Met	Tr	Met	Met	Tr	Met	Met	Tr	Met	Met	Tr	Met	Met	Tr
Fe	94.55	50.25	62.65	95.11	93.73	63.52	95.29	93.40	62.56	99.49	100.22	62.85	94.83	43.91	61.68
Co	0.22	0.08	0.00	0.39	0.30	0.00	0.36	0.15	0.01	0.13	0.07	0.04	0.46	0.01	0.07
Ni	5.03	48.77	0.00	4.16	5.08	0.00	3.94	6.74	0.14	0.05	0.14	0.00	4.29	54.27	0.08
Cr	0.00	0.00	0.00	0.00	0.00	0.00	0.01	0.01	0.05	0.00	0.00	0.03	0.04	0.00	0.02
S	0.00	0.00	37.57	0.00	0.00	36.47	0.00	0.00	36.17	0.04	0.02	36.23	0.00	0.11	37.47
Total	99.80	99.10	100.22	99.66	99.11	99.99	99.60	100.30	98.93	99.71	100.45	99.15	99.62	98.30	99.32

II-bearing enclaves						II-free enclaves									
Enclave 4632			Enclave 4630			Enclave 4633			Enclave 891			Enclave H			
	Met	Met	Tr	Met	Met	Tr	Met	Met	Tr	Met	Met	Tr	Met	Met	Tr
Fe	95.20	94.52	63.01	96.83	95.60	62.80	95.91	78.84	61.99	96.40	93.85	62.52	92.38	49.27	62.17
Co	0.26	0.36	0.00	0.31	0.49	0.00	0.53	0.49	0.00	0.48	0.52	0.00	0.51	0.11	0.00
Ni	4.21	4.22	0.00	2.90	3.51	0.02	3.39	19.61	0.10	3.44	5.50	0.13	6.76	49.34	0.15
Cr	0.00	0.04	0.01	0.04	0.04	0.05	0.00	0.00	0.04	0.00	0.00	0.01	0.06	0.01	0.03
S	0.06	0.02	36.64	0.00	0.03	36.50	0.04	0.06	36.37	0.00	0.00	36.09	0.00	0.00	36.67
Total	99.73	99.16	99.66	100.08	99.67	99.37	99.87	99.00	98.50	100.32	99.87	98.75	99.71	98.73	99.02

are below detection limits and extremely depleted in comparison with those in Il-bearing enclaves.

4.9. Troilite and Fe-Ni metal

Troilite and Fe-Ni metal are found in all of the samples, but the amounts are less than a few percent. Troilite is more abundant than Fe-Ni metal, and most Fe-Ni metal changes to Fe-hydrates by terrestrial alteration. Chemical compositions of

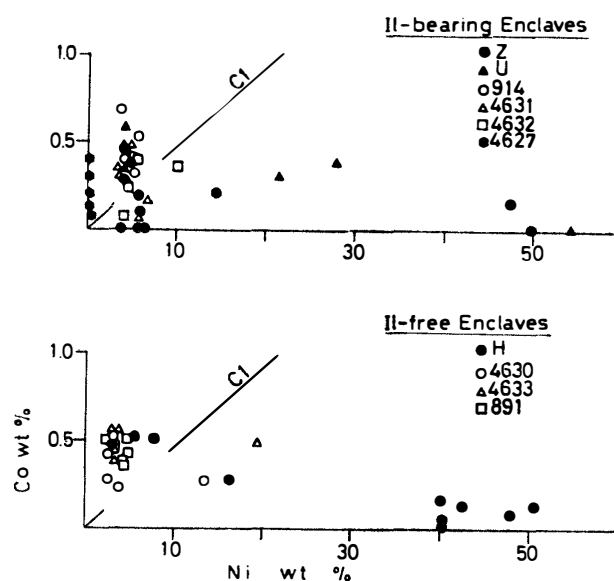


Fig. 27. Co and Ni (wt %) in Fe-Ni metal. The straight line labelled CI shows the Co/Ni ratio of CI chondrites (ANDERS and EBIHARA, 1982). Note that eucritic sample 4627 is extremely depleted in Ni.

Table 7. Summary of major petrographic characteristics of the Il-bearing and Il-free enclaves.

	Il-bearing group	Il-free group
Grain size	medium to coarse	coarse
Texture	porphyritic, subophitic, gabbroic	granular, gabbroic
Mineralogy		
Pigeonite	more ferroan (<i>mg</i> , 30–47)	more magnesian (<i>mg</i> , 43–64)
Opx	usually absent	usually present (<i>mg</i> , 50–66)
Ol	sometimes present	always absent
Plag	more sodic (An_{82-94})	more calcic (An_{91-98})
Ilmenite	always present	always absent
Chromite	Ti-rich	Ti-poor
Rutile	sometimes present	always absent
Zircon	sometimes present	always absent
Phosphate	whitlockite and sometimes fluorAp	always whitlockite
Exsolution in Pigeonite	weak or moderate	moderate
Subsolidus reduction	usually absent	usually present
An-En trend	similar to non-cumulate eucrites	similar to, or more calcic than, cumulate eucrites

Fe-Ni metal and troilite are shown in Table 6 and Fig. 27.

There are no systematic differences in the Ni contents of Fe-Ni metal in Il-bearing and Il-free enclaves. However, Fe-Ni metal in enclaves from Vaca Muerta are mainly kamacite, and those in enclaves from Mt. Padbury are kamacite and taenite. Fe-metal in eucritic sample 4627 is extremely depleted in Ni content, which is similar to Fe-Ni metal in howardites (HEWINS, 1979; IKEDA and TAKEDA, 1985).

4.10. Summary

Major characteristics of petrography and mineral compositions on the ilmenite-bearing and ilmenite-free enclaves in mesosiderites are summarized in Table 7.

Generally, the Il-bearing group has porphyritic, subophitic, or gabbroic textures, and has the characteristics of non-cumulate eucrites, suggesting they were formed from eucritic magmas. On the other hand, the Il-free enclaves have more or less granular textures, and have characteristics of cumulate eucrites, suggesting that they may have been produced as cumulates or residues.

5. Discussion

5.1. Crystallization

Figure 28 shows that the Il-bearing enclaves, and sample 4627, plot on the alkali-poor trend (trend A) similar to the main group eucrites. On the other hand, two Il-free enclaves (4633 and 891) plot on the cumulate eucrite trend (trend C), and two Il-free enclaves (H and 4630) plot slightly above the trend C. Pigeonite and plagioclase in enclave H are very magnesian with $mg=0.60-0.64$ and calcic with An_{95-98} , respectively. Using partition coefficients of 0.3 for MgO and FeO between pigeonite and silicate liquid (STOLPER, 1977), and the phase diagram of plagioclase (BOWEN, 1913), it is found that silicate liquid of $mg=0.31$ and An_{87} coexists with pigeonite of $mg=0.60$ and plagioclase of An_{96} . Therefore, a silicate liquid corresponding to enclave Z can coexist with a residue (or cumulate) corresponding to enclave H. The same consideration indicates that the other Il-free enclaves (4633 and 891) can coexist with a

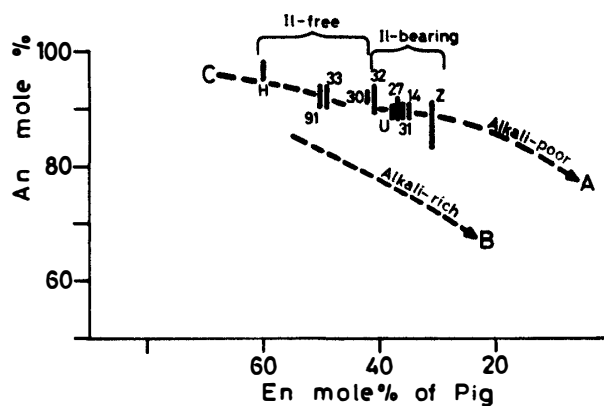


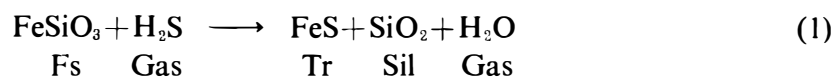
Fig. 28. Anorthite (mole %) of plagioclase plotted against enstatite (mole %) of pigeonite. Trends A, B, and C are alkali-poor, alkali-rich, and cumulate-eucrite trends of HED meteorites, respectively (IKEDA and TAKEDA, 1985).

liquid corresponding to trend B.

Chromites in enclaves also show a trend very similar to that of chromites in howardites (Fig. 25). Ulvospinel molecule components of Il-bearing enclaves are higher than those of Il-free enclaves, and the $2\text{Ti}/(\text{Al}+\text{Cr}+2\text{Ti})$ atomic percents range from 10 to 31 for the former, and from 0 to 17 for the latter (Table 3). The atomic percents tend to increase with decreasing *mg* values, suggesting that TiO_2 behaves as an incompatible element.

5.2. Reduction

The peripheral portions of pigeonites in Il-free enclaves are more or less replaced by hypersthene (Figs. 20 and 21). The hypersthene is more magnesian than the replaced pigeonites, but the CaO contents of the former are nearly the same as those of the latter (Fig. 24). In addition, the hypersthene includes tiny grains of troilite and silica-mineral in various amounts whereas the replaced pigeonites do not (Fig. 22). These textural observations and chemical composition indicate that the hypersthene was not produced as inverted pigeonites but formed by a reaction to produce magnesian hypersthene, troilite and a silica-mineral from the pigeonites. The exsolution lamellae of augite in the replaced pigeonite extend into the replacing hypersthene, suggesting that the reaction took place in a subsolidus condition after the formation of augite exsolution lamellae. The reducing agent may have been H_2S , and the reaction equation is:

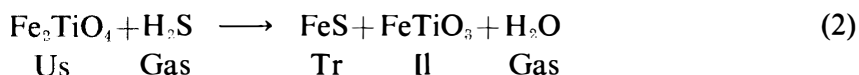


where Fs, Tr, and Sil are ferrosilite components in pigeonite, troilite, and silica-mineral, respectively. Instead of ferroan pigeonite, magnesian hypersthene was formed by replacement, a result of eq. (1). This reduction reaction probably took place before the mixing of the silicates and Fe-Ni metal to form mesosiderites, because pigeonites in the enclaves that are directly in contact with their host mesosiderite sometimes remain as pigeonites (Fig. 23) whereas pigeonites in the central portion of the enclaves are replaced by hypersthene. The replacement is often observed in coarse-grained Il-free enclaves in which the pigeonites include moderately-thick exsolution lamellae and rarely in fine-grained Il-bearing enclaves in which exsolution lamellae in the pigeonites are very thin, suggesting that the reduction took place intensely in deeper portions of the enclave parent body and slightly or not in shallower portions.

Enclave Z contains magnesian hypersthene in a fine-grained aggregate. The hypersthene is far more magnesian than the pigeonite phenocrysts (Fig. 24), and seems to coexist with magnesian augite, silica-mineral, and troilite which occur in the fine-grained aggregate. The two-pyroxene geothermometer (LINDSLEY and ANDERSEN, 1982) gives temperatures of 850° to 1000°C for the magnesian augite, and 900°C for magnesian hypersthene. As the solidus temperatures of eucritic magmas, with *mg* = about 0.4, are about 1080° – 1100°C (STOLPER, 1977), the temperatures of 850° – 1000°C determined for the fine-grained aggregates seem to be slightly lower than the solidus temperature of enclave Z, with *mg* = 0.39. This suggests that the fine-grained aggregates were equilibrated under subsolidus conditions. The magnesian hypersthene

and augite might have formed from clinopyroxene under reducing conditions.

Chromite in enclave Z is grouped into two types, TiO₂-rich and TiO₂-poor (Fig. 25). The latter occurs in fine-grained aggregates, and may have formed from TiO₂-rich chromites under reducing subsolidus conditions. A possible reaction equation is:



where Us and Il are ulvospinel molecule in chromite solid solution and ilmenite, respectively.

5.3. FeO-MnO relations

The FeO and MnO contents of clinopyroxene (pigeonite and augite), orthopyroxene (hypersthene), olivine, chromite, and ilmenite in each sample studied are shown in Fig. 29. Clinopyroxene in all enclaves has an FeO-MnO relationship similar to, or slightly higher in MnO than, that of HED meteorites. This is especially so for clinopyroxene in sample 4627 plotted for the typical trend of HED meteorites. Olivine in enclave Z is also similar in FeO-MnO relationship to ferroan olivine in howardites (IKEDA and TAKEDA, 1985). Hypersthene in enclave Z and in Il-free enclaves seems to have MnO contents similar to, or slightly higher than, clinopyroxene with the same FeO contents. The reaction in eq. (1) should increase the MnO content of hypersthene in comparison with ferroan pigeonite. However, the increase of MnO content by reaction (1) is small, because the difference in ferrosilite component between ferroan pigeonite and hypersthene (Fig. 24) is small, except for enclave Z. In addition, redistribution of MnO between newly-formed hypersthene and clinopyroxene might occur under subsolidus conditions.

On the other hand, chromite and ilmenite show a wide range of MnO contents (Fig. 29). In Fig. 30, the MnO contents of chromites in the enclaves studied are plotted against their MgO contents. Most chromites in the enclaves form an igneous trend from MgO-rich to MgO-poor, except for chromites in enclave 914, in the fine-aggregates of enclave Z, and rim chromite in enclave H, all of which have higher MnO than the trend.

In enclave Z, chromites show a bimodal distribution: chromites with MgO=0.4–0.7 wt% are Ti-rich and those with MgO=2.0–2.3 wt% are Ti-poor. As already noted in Section 4.5, the former are magmatic and the latter occur in the fine-grained aggregates and may be non-magmatic. The high contents of MnO and MgO of chromite and ilmenite in the fine-grained aggregates of enclave Z may be explained partly by reaction (2) for chromites, and partly by redistribution of MnO and MgO between these oxides and magnesian silicates which occur in the aggregates. Chromites in enclave H are zoned from Ti-poor core to Ti-rich rim. The core and rim are plotted in different portions of Fig. 30: the former is with MgO=2.9–3.1 wt%, and the latter with MgO=2.1–2.3 wt%. The rim chromites in enclave H are plotted in the same area as chromites in the fine-grained aggregates of enclave Z. They may be due to subsolidus redistribution of MnO and MgO under reduced conditions.

Chromites and ilmenites in enclave 914 are high in MnO (Fig. 29). Ilmenite in

enclave 914 is considered to have formed from ferropseudobrookite or armalcolite which became unstable at 1140°C, to form ilmenite and rutile intergrowths. The abnormally-high MnO content of ilmenites may come from the original phase, because rutile coexisting with the ilmenite is nearly free of MnO. The high MnO and MgO contents in the chromites may be due to the redistribution of these components between oxides and silicates.

5.4. Bulk compositions

The major element compositions of the silicate portions of the ten samples studied are shown according to STOLPER's method (STOLPER, 1977) in Fig. 31. The Il-free enclaves are richer in silica-mineral component in comparison with the cumulate eucrites, whereas all Il-bearing enclaves plot in the field of the non-cumulate eucrites. Three Il-bearing enclaves, Z, 914, and 4631 plot near the peritectic point of the pseudoternary system with $mg=0.40$. Il-bearing enclave U contains silica-mineral component in fairly large amount and may be near the pseudoternary eutectic point.

The silicate portions of mesosiderites have bulk compositions which differ from those in howardites (MITTFELDT, 1979); mesosiderites are richer in silica than howardites. The silica-rich nature of the mesosiderite silicate portions may be partly explained by the silica-rich nature of the eucritic component such as the enclaves studied here and partly by reduction of ferroan silicates by phosphorus derived from Fe-Ni metal after the mixing of metals and silicates.

5.5. REE contents

The trace element compositions of two Il-free enclaves, two Il-bearing enclaves, and the eucritic sample 4627 are shown in Table 8 and Fig. 32. The two Il-bearing enclaves (4631 and 4632) have moderate positive Eu-anomalies; the chondrite-normalized Eu/Sm ratios of 4631 and 4632 are 2.22 and 1.88, respectively, and the REE patterns are similar to those of the basalts of RUBIN and JERDE (1988). The two Il-free enclaves (4630 and 4633) have low REE contents with remarkable positive Eu-anomalies; the chondrite-normalized Eu/Sm ratio of 4630 is 13.6, and the patterns are similar to the gabbros of RUBIN and JERDE (1988).

As already noted, some whitlockites in enclaves 4631, U, and 4632 have suffered terrestrial alteration to change the Y_2O_3 and Ce_2O_3 contents and Ce/Y ratios (Fig. 26). Among the REEs, Eu is considered to reside mostly in plagioclases which are fresh in the enclaves, and the other REEs may be included in whitlockites which have been more or less altered. Therefore, the REE contents and the patterns of the bulk samples, except for Eu, may be affected by terrestrial alteration, although the degree of the effect is not known.

Here, two extreme cases are considered: (A) The REE contents of bulk enclaves did not change during terrestrial weathering although the whitlockites have suffered the alteration, and (B) the REE contents of bulk enclaves, except for Eu, have been depleted during terrestrial weathering and the original REE contents of the Il-bearing and Il-free enclaves were similar to those of non-cumulate eucrites (such as Juvinus or Pasamonte) and cumulate eucrites (such as Moore County), respectively. Juvinus and Pasamonte show flat REE patterns, and the Eu contents are about 9–10× chondrite

ILMENITE-BEARING ENCLAVES

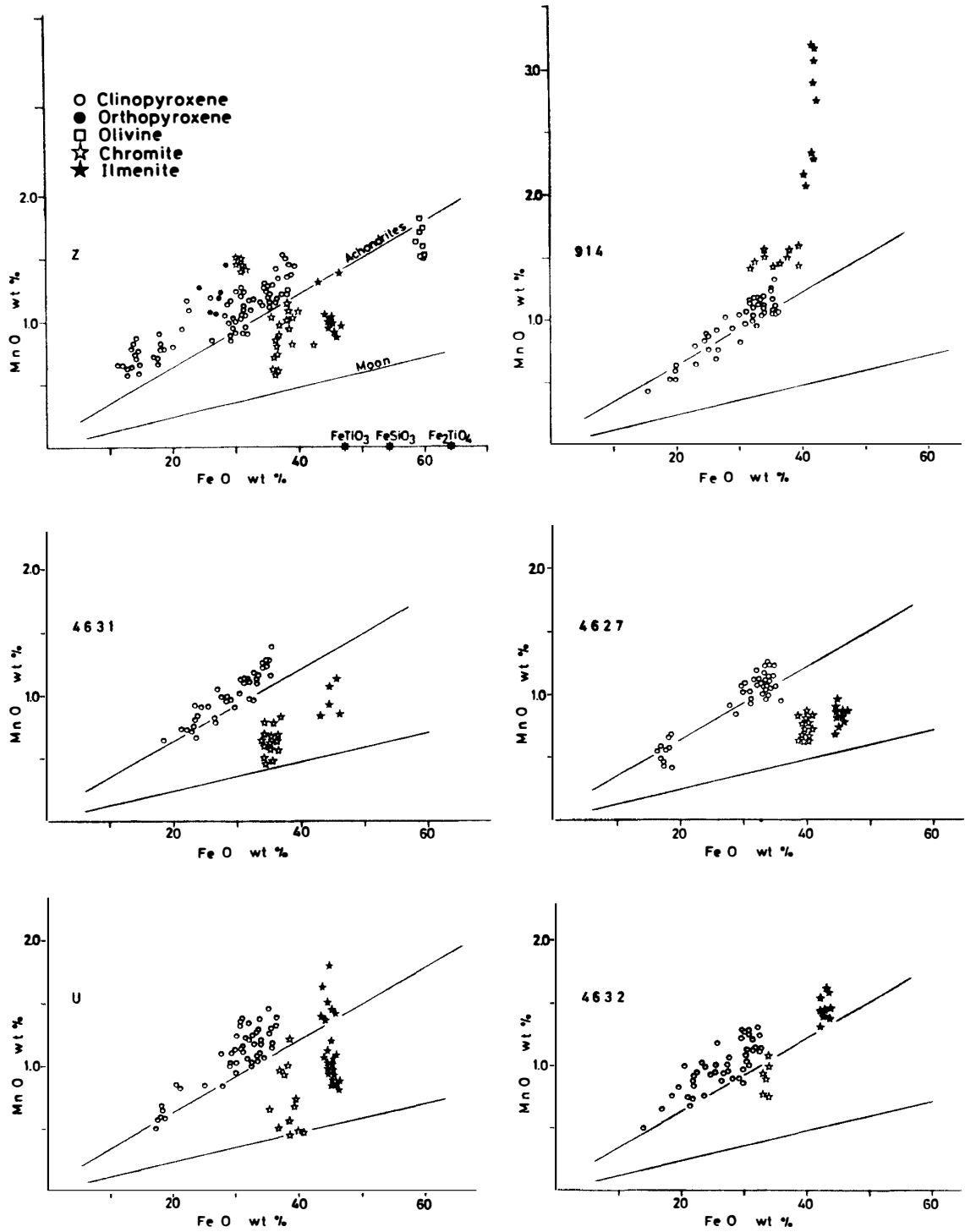


Fig. 29. MnO and FeO (wt%) of clinopyroxene (open circle), orthopyroxene (solid circle), olivine (open square), chromite (open star), and ilmenite (solid star). Note that chromites in enclave Z show a bimodal distribution: low-MnO chromites with high FeO and high-MnO chromites with low FeO. The latter occurs in the fine-grained aggregates and is low in Ti.

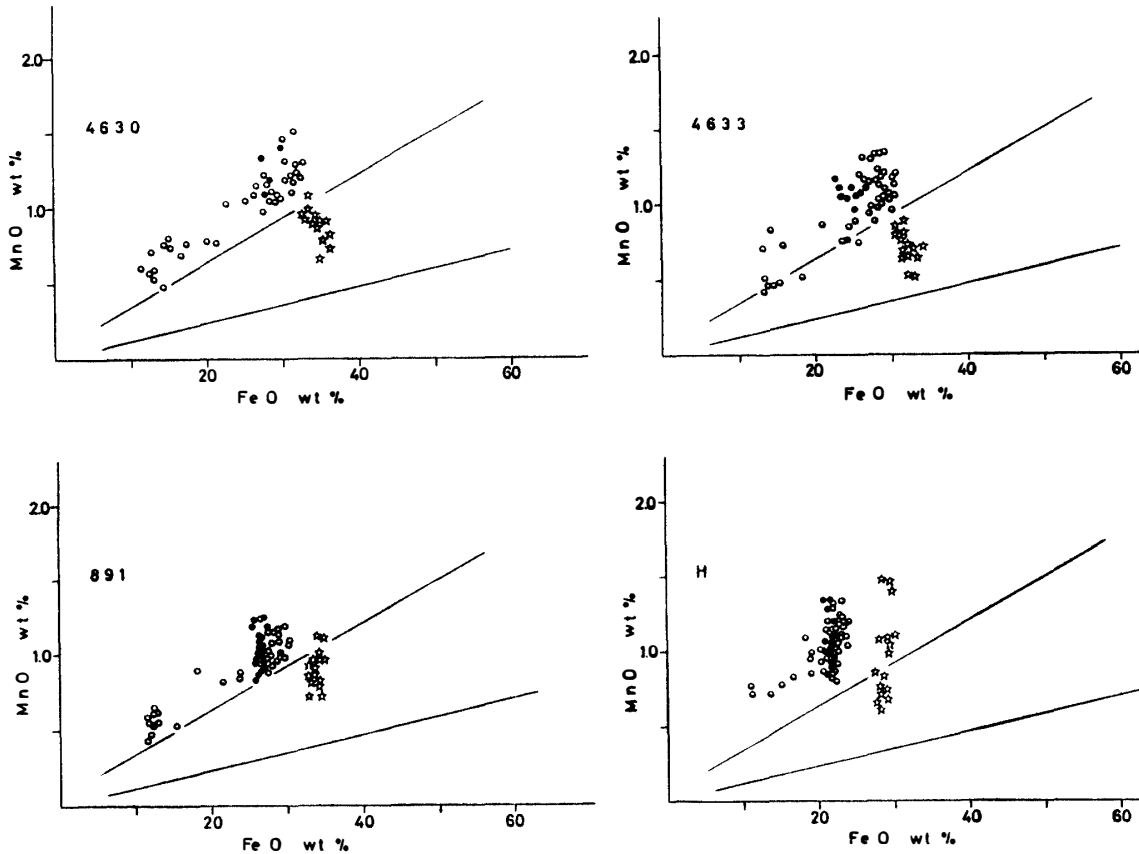
ILMENITE-FREE ENCLAVES

Fig. 29.

(CONSOLMAGNO and DRAKE, 1977) and similar to those of the Il-bearing enclaves 4631 and 4632. Moore County shows a moderate positive Eu-anomaly with a relatively-flat other-REE pattern of $4-5\times$ chondrite (CONSOLMAGNO and DRAKE, 1977) and the Eu content is similar to those of the Il-free enclaves 4630 and 4633.

If the former case (A) is true, the positive Eu-anomalies of the Il-bearing eucritic enclaves are remarkable in contrast to the flat REE patterns of the non-cumulate eucrites, and those of the Il-free enclaves are surprisingly steep in comparison with the cumulate eucrites. RUBIN and JERDE (1987, 1988) explained these facts by the idea that "basaltic clasts", which correspond to the Il-bearing enclaves, were produced by total melting of eucritic basalts with lesser amount of cumulate eucritic rocks, and that the "gabbroic clasts", which correspond to the Il-free enclaves, were produced as residues by partial melting of cumulate gabbros. However, the source materials for the Il-free enclaves should be enriched in silica-mineral component in comparison with the cumulate eucrites. The Il-bearing enclaves have chemical compositions similar to those of the peritectic liquid (Fig. 31), suggesting that they are not a mixture of eucritic basalts and cumulate eucritic rocks. The Il-bearing enclaves could be produced as eutectic or peritectic liquids by partial melting of quartz-plagioclase-pyroxene or olivine-plagioclase-pyroxene cumulative rocks, and the Il-free enclaves could be produced as residues by partial melting of silica-rich cumulative gabbros.

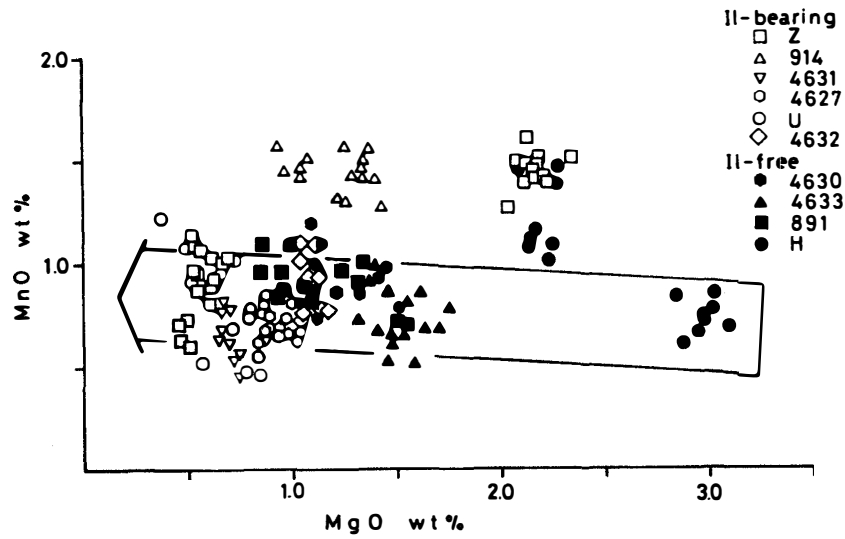


Fig. 30. *MnO and MgO (wt %) of chromites. A large arrow shows the magmatic trend of chromites. Note that chromites in enclaves Z and H show bimodal distributions: chromites in enclave Z with $MgO = 0.4-0.7$ and $2.0-2.3$ (wt %) occur in the main portion and in the fine-grained aggregates, respectively. Chromites in enclave H with $MgO = 2.9-3.1$ and $2.1-2.3$ (wt %) occur as the core and rim of chromite grains, respectively.*

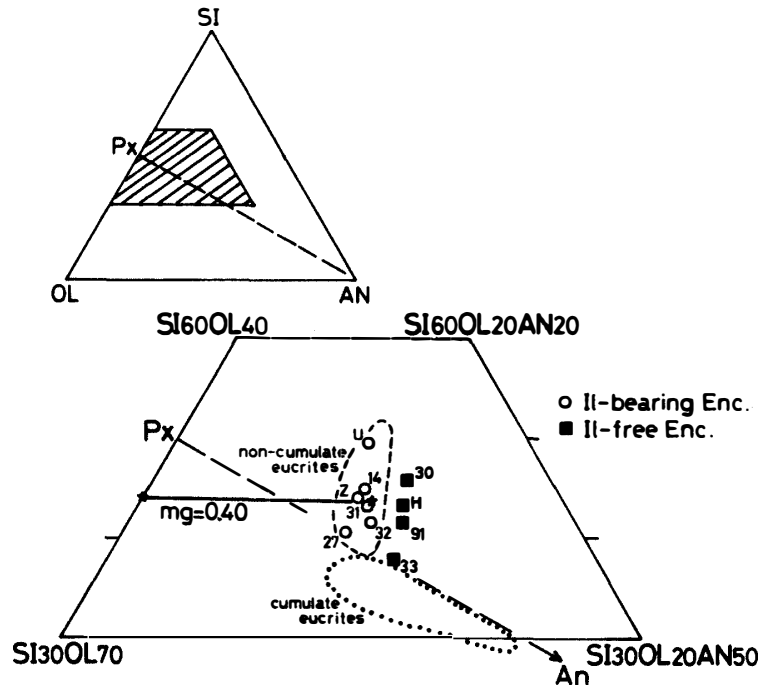


Fig. 31. *Mole ratios of olivine (OL), anorthite (AN), and silica (SI) plotted according to STOLPER'S method (STOLPER, 1977). Il-bearing samples and Il-free enclaves are shown by open circles and solid squares, respectively. The compositional ranges of non-cumulate and cumulate eucrites (MASON et al., 1979) are shown by the fields surrounded by dashed and dotted lines, respectively. The straight line, with $mg = 0.40$, is the assumed boundary between olivine and pyroxene liquidus fields for eucritic magmas (IKEDA and TAKEDA, 1985), and a solid star is the peritectic point (STOLPER, 1977).*

Table 8. INAA and RNAA data for two Il-bearing enclaves (4631 and 4632), two Il-free enclaves (4630 and 4633), and a eucritic sample 4627. The concentrations are given in wt% for major elements (Fe and Na) and in ppm for trace elements.

	Chile 4627	V. M. 4630	V. M. 4631	V. M. 4632	V. M. 4633
INAA					
Fe (%)	15.4	14.2	14.6	14.4	13.7
Na (%)	0.35	0.30	0.38	0.31	0.24
Sr (ppm)	101				
Ba	334	<14	<27	<14	<12
Sc	32.2	30.0	28.6	25.0	27.0
Hf	0.94		0.79	0.45	
Cr	1700	2040	1180	2030	1890
Ni	10	1480	214	2290	797
Co	5.34	49.1	12.6	67.6	41.9
RNAA					
La	2.54	0.129	1.12	1.12	0.0866
Ce	6.69		3.03	3.19	0.217
Nd	4.95		1.71	2.06	0.212
Sm	1.5	0.0782	0.677	0.676	
Eu	0.549	0.407	0.576	0.486	0.389
Gd	2.3		1.4	1.27	
Tb	0.373	0.0233	0.242	0.202	0.0262
Tm	0.228	0.0204	0.172	0.124	
Yb	1.72	0.268	1.39	0.961	
Lu	0.272	0.0409	0.197	0.143	0.0227

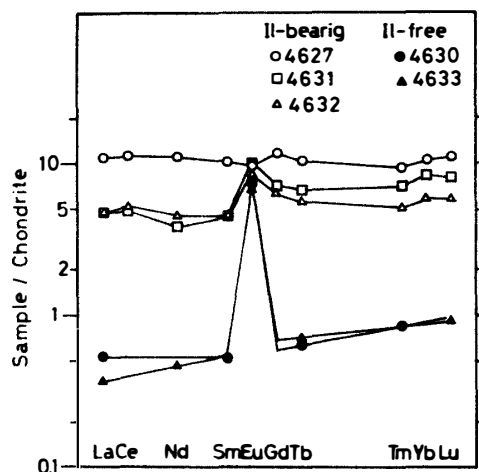


Fig. 32. Trace element concentrations of five eucritic enclaves (Il-bearing: 4627, 4631, 4632, Il-free; 4630, 4633) normalized to CI chondrites (Orgueil) and Si.

If the case (B) is true, the above-stated scenario should be changed. The Il-bearing enclaves could be produced in the similar way to those of non-cumulate eucrites. Non-cumulate eucrites are classified into three groups on the basis of bulk chemical composition; main group, Nuevo Laredo trend and Stannern trend eucrites (STOLPER, 1977; BVSP, 1981). The main group and Nuevo Laredo trend eucrites are considered to be produced by fractional crystallization of ultramafic magmas (IKEDA and TAKEDA, 1985), and Stannern trend eucrites are considered to be produced by partial melting of a source material (STOLPER, 1977). Eucrites belonging to the main group and Nuevo

Laredo trend form trend A in Fig. 28, and the Il-bearing enclaves are also plotted on the same trend, suggesting that they are eucritic rocks similar to the main group or Nuevo Laredo trend. However, the common presence of zircon and rutile in the Il-bearing enclaves suggests that incompatible elements such as Ti and Zr concentrated efficiently by partial melting of a source material and they could be produced in the same way as the Stannern trend eucrites. The Il-free enclaves could be produced as cumulates or residues. If they were produced as cumulates from a eucritic magma, the eucritic magma should have been crystallizing silica-mineral in addition to pyroxene and plagioclase to produce the Il-free enclaves, because the Il-free enclaves are richer in silica-mineral in comparison with the cumulate eucrites. If they were produced as residues, the source material should be enriched in silica-mineral.

Recently, it was found that some Antarctic eucritic meteorites are depleted in REEs except for Eu during terrestrial weathering (T. FUKUOKA, 1989, oral commun.); the REE contents of peripheral portions of a eucritic meteorite are lower by a factor less than 2 in comparison with those of the interior. Therefore, we prefer the case (B) to the case (A), but the REE contents of the Il-free enclaves, except for Eu, are depleted by a factor of 4–8 in comparison with those of the Moore County eucrite. Further study should be done for the conclusion.

6. Origin of Enclaves

The evidence presented, including igneous textures, major element chemical compositions, REE contents, *etc.*, indicates that the Il-bearing and Il-free enclaves are magmatic and residual (or cumulative) rock types, respectively.

There are significant differences between eucrites and eucritic enclaves. Il-bearing enclaves have medium-grained doleritic or coarse-grained gabbroic textures, whereas most maingroup eucrites have fine-grained basaltic textures. The Il-free enclaves contain more abundant silica-mineral component than cumulate eucrites.

Reduction of ferroan pigeonites by H_2S to form hypersthene under subsolidus conditions is a remarkable feature of the Il-free enclaves, whereas such reduction is never observed in HED meteorites. The reduction probably took place in the interior of the enclave parent body. The MnO/FeO ratios of pyroxene in the enclaves seem to be slightly higher, on average, than those of the HED meteorites.

In conclusion, eucritic enclaves from mesosiderites were formed in a parent body which is different from the HED parent body, in spite of the fact that mesosiderites and HED meteorites have similar oxygen isotopic composition (CLAYTON *et al.*, 1976).

Eucritic sample 4627 has a coarse-grained gabbroic texture which is similar to that of some enclaves from mesosiderites. However, there are several significant differences between sample 4627 and the Il-bearing enclaves. (1) Mineralogical differences: the Ni content of metals in sample 4627 is extremely low in comparison to that in the enclaves, and it has the least amount of silica-mineral. (2) Differences in bulk composition: in contrast to the positive Eu-anomalies for Il-bearing enclaves, the flat REE pattern and REE content of sample 4627 are very similar to those of the non-cumulate eucrites, as is the major element composition. (3) Fusion crust completely surrounds sample 4627, whereas the eucritic enclaves are surrounded by the host mesosiderite.

These facts suggest that sample 4627 is not an enclave but an independent eucritic meteorite, although an enclave origin cannot be completely ruled out.

7. Conclusions

- (1) Eucritic sample AMNH 4627 may be an independent eucritic meteorite.
- (2) Eucritic enclaves in mesosiderites have crystallization trends of pyroxene, plagioclase, and chromite that are similar to those of HED meteorites.
- (3) Whitlockite has a higher REE content than that in coexisting fluorapatite. Whitlockite of the Il-bearing enclaves is much higher in REE content than that in Il-free enclaves. Some whitlockite has suffered terrestrial alteration and changed its REE pattern.
- (4) Rutile and ilmenite intergrowths in enclave 914 may have formed by decomposition from ferropseudobrookite or armalcolite. Zircon occurs in an enclave from Mt. Padbury.
- (5) Il-free enclaves suffered reduction by H_2S under subsolidus conditions to produce magnesian orthopyroxene from ferroan pigeonitic pyroxene, prior to formation of the mesosiderites. An Il-bearing enclave (Z) also suffered reduction by H_2S at sub-solidus temperatures to produce magnesian hypersthene from pigeonite in fine-grained aggregates.
- (6) The Il-bearing enclaves show moderate positive Eu-anomalies with chondrite-normalized Eu/Sm ratios of 1.88–2.22, and the Il-free enclaves are extremely depleted in REEs and show remarkable positive Eu-anomalies with Eu/Sm ratios of 13.6. The high ratios seem to be partly due to terrestrial weathering. On the other hand, eucritic sample 4627 shows a flat REE pattern with no Eu-anomaly similar to that of main group eucrites.
- (7) Il-bearing enclaves represent eutectic or peritectic magmas, and are similar in bulk chemical composition to non-cumulate eucrites. Il-free enclaves represent eucritic residues or cumulates, and are richer in the silica-mineral component than the cumulate eucrites. If they are residues, the source material may be silica-rich gabbros which differ from the cumulate eucrites. If they are cumulates, the magmas should be silica-rich liquid near the pseudoternary eutectic point.
- (8) The silica-rich bulk composition of mesosiderite silicates than howartides are partly due to the silica-rich nature of the eucritic component.
- (9) The silica-rich nature of the eucritic enclaves and reduction of pigeonites in the Il-free enclaves suggest that the parent body for the enclaves in mesosiderites differs from the HED parent body.

Acknowledgments

We thank Prof. H. TAKEDA for his discussions. This work was supported by NASA grant NAG 9-32 (M. PRINZ, P. I.).

References

- AGOSTO, W. H., HEWINS, R. H. and CLARKE, R. S., Jr. (1980): Allan Hills A77219, the first Antarctic mesosiderite. *Proc. Lunar Planet. Sci. Conf.*, 11th, 1027–1045.
- ANDERS, E. and EBIHARA, M. (1982): Solar-system abundances of the elements. *Geochim. Cosmochim. Acta*, **46**, 2363–2380.
- ANDO, A., MITA, N. and TERASHIMA, S. (1987): 1986 values for fifteen GSJ rock reference samples, “igneous rock series”. *Geostand. Newslett.*, **11**, 159–166.
- BASALTIC VOLCANISM STUDY PROJECT (1981): *Basaltic Volcanism on the Terrestrial Planets*. New York, Pergamon Press.
- BOWEN, N. L. (1913): The phenomena of the plagioclase feldspars. *Am. J. Sci.*, **35**, 577–599.
- CLAYTON, R. N., ONUMA, N. and MAYEDA, T. (1976): A classification of meteorites based on oxygen isotopes. *Earth Planet. Sci. Lett.*, **30**, 10–18.
- CONSOLMAGNO, G. J. and DRAKE, M. J. (1977): Composition and evolution of the eucrite parent body; Evidence from rare earth elements. *Geochim. Cosmochim. Acta*, **41**, 1271–1282.
- DELANEY, J. S., NEHRU, C. E., PRINZ, M. and HARLOW, G. E. (1981): Metamorphism of mesosiderites. *Proc. Lunar Planet. Sci. Conf.*, 12th, 1315–1342.
- DELANEY, J. S., HARLOW, G. E., NEHRU, C. E., O’NEILL, C. and PRINZ, M. (1982): Mount Padbury mafic “enclaves” and the petrogenesis of mesosiderite silicates. *Lunar and Planetary Science XIII*. Houston, Lunar Planet. Inst., 152–153.
- DESNOYERS, C. (1982): L’Olivine dans les howardites; Origine, et implications pour le corps parent de ces meteorites achondritiques. *Geochim. Cosmochim. Acta*, **46**, 667–680.
- DUKE, M. B. and SILVER, L. T. (1967): Petrology of eucrites, howardites and mesosiderites. *Geochim. Cosmochim. Acta*, **31**, 1637–1665.
- EBIHARA, M. (1987): Determination of ten lanthanoids in chondritic meteorites by radiochemical neutron activation analysis using coaxial and planar type Ge detectors. *J. Radioanal. Nucl. Chem.*, **111**, 385–397.
- FLORAN, R. J. (1978): Silicate petrography, classification, and origin of the mesosiderites; Review and new observations. *Proc. Lunar Planet. Sci. Conf.*, 9th, 1053–1081.
- HARLOW, G. E., DELANEY, J. S., NEHRU, C. E. and PRINZ, M. (1982): Metamorphic reactions in mesosiderites; Origin of abundant phosphate and silica. *Geochim. Cosmochim. Acta*, **46**, 339–348.
- HEWINS, R. H. (1979): The composition and origin of metal in howardites. *Geochim. Cosmochim. Acta*, **43**, 1663–1673.
- IKEDA, Y. and TAKEDA, H. (1985): A model for the origin of basaltic achondrites based on the Yamato 7308 howardite. *Proc. Lunar Planet. Sci. Conf.*, 15th, Part 2 (*J. Geophys. Res.*, **90**), C649–C663.
- JAROSEWICH, E., CLARKE, R. S., Jr. and BARROWS, J. (1987): The Allende meteorite reference sample. *Smithson. Contrib. Earth Sci.*, **27**, 1–12.
- LINDSLEY, D. H. (1965): *Iron-Titanium Oxides*. Washington, D. C., Carnegie Inst., Year Book 64, 144–148.
- LINDSLEY, D. H. and ANDERSEN, D. J. (1982): A two-pyroxene thermometer. *Proc. Lunar Planet. Sci. Conf. 13th, Part 2 (J. Geophys. Res.*, **88**), A887–A906.
- MARVIN, U. B. and KLEIN, C., Jr. (1964): Meteoritic zircon. *Science*, **146**, 919–920.
- MASON, B., JAROSEWICH, E. and NELEN, J. A. (1979): The pyroxene-plagioclase achondrites. *Smithson. Contrib. Earth Sci.*, **22**, 27–45.
- MCCALL, G. J. H. (1966): The petrology of the Mount Padbury mesosiderite and its achondrite enclaves. *Mineral. Mag.*, **35**, 1029–1060.
- MITTFEHLDT, D. W. (1979): Petrographic and chemical characterization of igneous lithic clasts from mesosiderites and howardites and comparison with eucrites and diogenites. *Geochim. Cosmochim. Acta*, **43**, 1917–1935.
- MITTFEHLDT, D. W., CHOU, C.-L. and WASSON, J. T. (1979): Mesosiderites and howardites; Igneous formation and possible genetic relationships. *Geochim. Cosmochim. Acta*, **43**, 673–688.

- NEHRU, C. E., DELANEY, J. S., HARLOW, G. E. and PRINZ, M. (1980): Mesosiderite basalts and eucrites. *Meteoritics*, **15**, 337–338.
- POWELL, B. N. (1971): Petrology and chemistry of mesosiderites—II; Silicate textures and compositions and metal-silicate relationships. *Geochim. Cosmochim. Acta*, **35**, 5–34.
- RUBIN, A. E. and JERDE, E. A. (1987): Diverse eucritic pebbles in the Vaca Muerta mesosiderite. *Earth Planet. Sci. Lett.*, **84**, 1–14.
- RUBIN, A. E. and JERDE, E. A. (1988): Compositional differences between basaltic and gabbroic clasts in mesosiderites. *Earth Planet. Sci. Lett.*, **87**, 485–490.
- SIMPSON, A. B. and AHRENS, L. H. (1979): The Mg-Cr relationship in achondrites and in the silicate fraction of mesosiderites, and additional observations on eucrites. *Meteoritics*, **14**, 215–232.
- STOLPER, E. (1977): Experimental petrology of eucritic meteorites. *Geochim. Cosmochim. Acta*, **41**, 587–611.

(Received September 5, 1989; Revised manuscript received January 23, 1990)